

December 2002

rhad: a program for the evaluation of the hadronic R -ratio in the perturbative regime of QCD

Robert V. Harlander^a and Matthias Steinhauser^b

(a) Theory Division, CERN, CH-1211 Geneva 23, Switzerland

(b) II. Institut für Theoretische Physik,
Universität Hamburg, D-22761 Hamburg, Germany

Abstract

This paper describes the `fortran` program `rhad` which performs a numerical evaluation of the photon-induced hadronic R -ratio, $R(s)$, related to the cross section for electron-positron annihilation, for a given center-of-mass energy \sqrt{s} . In `rhad` the state-of-the-art perturbative corrections to $R(s)$ are implemented and the running and decoupling of the strong coupling constant and the quark masses is automatically treated consistently. Several options allow for a flexible use of the program.

PROGRAM SUMMARY

Title of program: rhad

Available from:

<http://www.rhad.de/>

Computer for which the program is designed and others on which it is operable: Any work-station or PC where **fortran** is running.

Operating system or monitor under which the program has been tested: Alpha, Linux, Solaris

No. of bytes in distributed program including test data etc.: 168000

Distribution format: ASCII

Keywords: Hadronic R -ratio, perturbative QCD, electron-positron annihilation, running and decoupling of α_s

Nature of physical problem: The hadronic R -ratio $R(s)$ is a fundamental quantity in high energy physics. It is defined as the ratio of the inclusive cross section $\sigma(e^+e^- \rightarrow \text{hadrons})$ and the point cross section $\sigma_{pt} = 4\pi\alpha^2/(3s)$. It is well-defined both from the experimental and the theoretical side. $R(s)$ belongs to the few physical quantities for which high-order perturbative calculations have been performed (partial results up to order α_s^4 exist!). Mass effects from real and virtual quarks, the evolution of the $\overline{\text{MS}}$ parameters, in particular in the presence of thresholds, and other subtleties lead to fairly complex results in high orders. Thus it is important to provide a comprehensive collection of formulas in order to make them available to non-experts.

Method of solution: **rhad** is a compilation of all currently available perturbative QCD corrections to the quantity $R(s)$. Several options are provided which allow for a flexible use. In addition, **rhad** contains routines which perform the running and decoupling of the strong coupling constant. Thus only the center-of-mass energy has to be provided in order to determine $R(s)$.

Restrictions on the complexity of the problem: The applicability of **rhad** is restricted to the perturbative energy regions and does not cover the narrow and broad resonances.

Typical running time: The typical runtime is of the order of fractions of a second.

1 General structure of $R(s)$

We are considering the fully inclusive production of quark pairs in e^+e^- annihilation (for a review see Ref. [1]). The tree-level diagram for this process is shown in Fig. 1 (a). At leading order (LO) perturbative QCD (pQCD), the cross section as a function of the squared center-of-mass (c.m.s.) energy, s , has thresholds at the points $s = 4m_Q^2$ with $Q = d, u, s, c, b, t$. However, close to threshold, fixed-order pQCD is no longer applicable. Below threshold, non-perturbative effects lead to the formation of bound states of the quark–anti-quark pair, which appear as more or less sharp peaks in the cross section.¹ In our perturbative framework of charm and bottom production, these narrow resonances cannot be described, and are therefore not included in `rhad`. In addition, we have to spare out the region between the physical threshold s_Q^{low} and the beginning of the more or less flat continuum region at s_Q^{thr} , where the cross section exhibits rapid variations. In the case of charm production, for example, the limits would be $\sqrt{s_c^{\text{low}}} \approx 2m_D \approx 3.73$ GeV and $\sqrt{s_c^{\text{thr}}} \approx 4.8$ GeV, while for bottom production they are $\sqrt{s_b^{\text{low}}} \approx 2m_B \approx 10.52$ GeV and $\sqrt{s_b^{\text{thr}}} \approx 11.2$ GeV. Even though `rhad` provides a numerical value in these threshold regions, one should not try to give this value any physical significance; `rhad` will print a warning that reminds the user of this fact.

Furthermore, we have to exclude the low-energy region, below about $\sqrt{s_{\text{min}}} = 1.8$ GeV, where the validity of perturbation theory is doubtful. Thus, mass effects from u -, d - and s -quarks are negligible, which is why we will consider these quarks as massless throughout the paper.

Instead of the cross section $\sigma(e^+e^- \rightarrow \text{hadrons})$, we will express the results in terms of the so-called hadronic R -ratio,

$$R(s) = \frac{\sigma(e^+e^- \rightarrow \text{hadrons})}{\sigma(e^+e^- \rightarrow \mu^+\mu^-)}, \quad (1)$$

where

$$\sigma(e^+e^- \rightarrow \mu^+\mu^-) = \frac{4\alpha^2\pi}{3s} \quad (2)$$

is the high-energy limit for the photon-mediated lowest order muon pair production. In this paper we concentrate on the contributions induced by photon exchange. Z -boson exchange is only relevant at high energies. There, however, apart from the QCD corrections², also the electro-weak corrections become important [2]; these will not be addressed in this paper. Nevertheless, `rhad` can be used to evaluate the vector contribution to the production of top quarks in the same way as for charm and bottom production.

We write $R(s)$ as a sum of contributions from individual quark flavors, plus a so-called

¹Due to the large width no bound state is formed in the top quark system. However, a peak in the cross section remains around $s = 4m_t^2$.

²For a discussion of corrections to the axial-vector correlator see Ref. [1].

singlet term:

$$R(s) = \sum_{Q=d,u,s,c,b,t} R_Q(s) + R_{\text{sing}}(s). \quad (3)$$

The “non-singlet” contributions $R_Q(s)$ are all proportional to the square of the respective quark charge. The (numerically small) singlet piece R_{sing} appears for the first time at order α_s^3 and will be discussed in Sect. 6.

$R_Q(s)$ is defined to be zero below the continuum region of $Q\bar{Q}$ production (s_Q^{thr}), *i.e.*, we do not attempt to describe the resonance regime:

$$R_Q(s < s_Q^{\text{thr}}) = 0. \quad (4)$$

Our main concern are the radiative corrections to $R_Q(s)$, predominantly arising from gluons exchanged between, or emitted from, the $Q\bar{Q}$ pair, but the lowest order QED effects, though very small, will also be included. Thus we write

$$R_Q(s) = \theta(s - s_Q^{\text{thr}}) \left[\sum_{n \geq 0} \left(\frac{\alpha_s}{\pi} \right)^n R_Q^{(n)}(s) + \delta R_Q^{\text{QED}}(s) \right]. \quad (5)$$

This formula generally describes the QCD/QED effects to $R_Q(s)$, if $\delta R_Q^{\text{QED}}(s)$ contains all contributions that vanish when electro-magnetic corrections are ignored. Both α_s and $R_Q^{(n)}(s)$ explicitly depend on the renormalization scale μ , while $R_Q(s)$ is invariant under μ -variation, up to and including the order of perturbation theory that is being considered.

Since the QCD corrections only affect the quarks in Fig. 1 (a), the leptonic part of the diagrams can be factored out and one remains with corrections to the $\gamma Q\bar{Q}$ vertex, and real radiation of quarks and gluons. Beyond order α_s , the most convenient way to evaluate the fully inclusive rate is to compute the photon self energy and relate it to the rate $\gamma^* \rightarrow Q\bar{Q} + X$ through the optical theorem, *i.e.*, by taking the imaginary part in the time-like region of the external momentum. Explicitly,

$$R(s) = 12\pi \text{Im}\Pi(s + i\epsilon), \quad (6)$$

where

$$\Pi(q^2) = \frac{1}{3q^2} \left(-g_{\mu\nu} + \frac{q_\mu q_\nu}{q^2} \right) \Pi_{\mu\nu}(q) \quad (7)$$

is the transversal part of the photon polarization function, $\Pi_{\mu\nu}(q)$.

The different contributions to $R(s)$, as we classify them in our paper, will be illustrated by sample diagrams contributing to $\Pi(q^2)$ in what follows. The LO terms are thus represented by Fig. 1 (b). Since the imaginary part of these diagrams is obtained by the sum of all possible cuts, it includes real and virtual contributions simultaneously.

A final remark concerning the counting of loops is in order. We understand by the n -loop QCD contribution to $R(s)$ the sum of real and virtual corrections to order α_s^n . Computing $R(s)$ via the optical theorem at n -loop level thus requires the evaluation of the imaginary part of the photon self-energy to $n + 1$ loops.

2 Running and decoupling of α_s and the quark masses

As already mentioned in the previous section, the quantity $R(s)$ depends on the strong coupling constant α_s , the heavy quark masses m_Q , and the renormalization scale μ . All of them are specified in the subroutine `parameters` which is discussed in Appendix C. The dependence of $R(s)$ on μ is explicit in terms of logarithms, but also implicit as, for example, in the argument of α_s . At higher orders in perturbation theory, one needs to specify the scheme in which α_s and the quark masses m_Q are evaluated. For α_s , we will always adopt the $\overline{\text{MS}}$ scheme which is commonly used in QCD calculations. Concerning the quark masses, it is generally more appropriate to use the pole mass in the energy region close to the production threshold of the quarks. On the other hand, the use of the running mass and setting $\mu^2 = s$ resums part of the potentially large logarithms $\ln m_Q^2/s$ in the high-energy region. For this reason, `rhad` provides the logical parameter `lmsbar` that allows the user to switch between the pole and the $\overline{\text{MS}}$ mass definition for the evaluation of $R(s)$. If not stated otherwise, we denote by m_Q a generic quark mass in what follows. In those cases where it is necessary to distinguish between the pole and $\overline{\text{MS}}$ quark mass, we denote them by M_Q and $\bar{m}_Q \equiv \bar{m}_Q^{(n_f)}(\mu)$, respectively. The conversion formula between M_Q and \bar{m}_Q is given in App.E.4, Eq. (67). The “scale-invariant” mass is defined recursively as $\bar{m}_Q(\bar{m}_Q) \equiv \bar{m}_Q^{(n_f)}(\bar{m}_Q^{(n_f)})$, where the number of active flavors is equal to $n_f = 4$ for charm, $n_f = 5$ for bottom, and $n_f = 6$ for top quarks.

If one chooses to evaluate $R(s)$ in terms of $\overline{\text{MS}}$ masses, the input required by `rhad` is $\alpha_s^{(5)}(M_Z)$ and the scale invariant masses $\bar{m}_Q(\bar{m}_Q)$ ($Q = c, b, t$). In addition, one needs to specify the renormalization scale μ and the c.m.s. energy squared, s . From that, `rhad` will determine the number of active flavors n_f , as well as the parameters $\alpha_s^{(n_f)}(\mu)$ and $\bar{m}_Q^{(n_f)}(\mu)$, which will be used for the evaluation of $R(s)$. As already mentioned before, a natural choice (and the default value in `rhad`) for the renormalization scale is $\mu^2 = s$.

The number of active flavors is determined through the threshold variables s_c^{thr} , s_b^{thr} , and s_t^{thr} . When $s < s_c^{\text{thr}}$, it assumes the smallest possible value, $n_f = 3$, and it increases by one every time one of the threshold variables is crossed, up to $n_f = 6$ for $s > s_t^{\text{thr}}$.

On the other hand, in the definition of $\alpha_s^{(n_f)}(\mu)$ one has the freedom to choose “matching scales” μ_c , μ_b , and μ_t , at which the transition from n_f to $n_f \pm 1$ is performed. For example, assume that $n_f = 4$, and the renormalization scale is set to some specific value $\mu = \bar{\mu}$. The procedure to compute $\alpha_s^{(4)}(\bar{\mu})$ at n -loop order as implemented in `rhad` is as follows: In a first step the renormalization group equation (RGE) for the strong coupling (here and in what follows, we refer to App.E.4 for the definition of the coefficients β , ζ_g , γ_m , and ζ_m),

$$\mu^2 \frac{d}{d\mu^2} \frac{\alpha_s^{(n_f)}(\mu)}{\pi} = \beta^{(n_f)} \left(\alpha_s^{(n_f)}(\mu) \right) = - \sum_{i=0}^{n-1} \beta_i^{(n_f)} \left(\frac{\alpha_s^{(n_f)}(\mu)}{\pi} \right)^{i+2}, \quad (8)$$

is solved numerically in order to obtain $\alpha_s^{(5)}(\mu_b)$ from the input value $\alpha_s^{(5)}(M_Z)$. The use of the decoupling relation

$$\alpha_s^{(n_f-1)}(\mu_b) = (\zeta_g)^2 \alpha_s^{(n_f)}(\mu_b) \quad (9)$$

to $(n-1)$ -loop order, leads to $\alpha_s^{(4)}(\mu_b)$. Finally, applying Eq. (8) a second time gives the

value for $\alpha_s^{(4)}(\bar{\mu})$. The described procedure is performed automatically in `rhad` using the subroutine `rundecalalpha` (see App. D).

The evaluation of $\bar{m}_Q^{(n_f)}(\mu)$ from the input $\bar{m}_Q(\bar{m}_Q)$ proceeds completely analogously. The RGE that governs the running of the quark masses in the $\overline{\text{MS}}$ scheme reads:

$$\mu^2 \frac{d}{d\mu^2} \bar{m}_Q^{(n_f)}(\mu) = \bar{m}_Q^{(n_f)}(\mu) \gamma_m^{(n_f)} \left(\alpha_s^{(n_f)}(\mu) \right) = -\bar{m}_Q^{(n_f)}(\mu) \sum_{i \geq 0} \gamma_{m,i}^{(n_f)} \left(\frac{\alpha_s^{(n_f)}(\mu)}{\pi} \right)^{i+1}. \quad (10)$$

Combining Eqs. (8) and (10) leads to

$$\bar{m}_Q^{(n_f)}(\mu) = \bar{m}_Q^{(n_f)}(\mu_0) \frac{c(\alpha_s(\mu)/\pi)}{c(\alpha_s(\mu_0)/\pi)}, \quad (11)$$

with

$$\begin{aligned} c(x) = x^{c_0} & \left\{ 1 + (c_1 - b_1 c_0) x + \frac{1}{2} [(c_1 - b_1 c_0)^2 + c_2 - b_1 c_1 + b_1^2 c_0 - b_2 c_0] x^2 \right. \\ & + \left[\frac{1}{6} (c_1 - b_1 c_0)^3 + \frac{1}{2} (c_1 - b_1 c_0) (c_2 - b_1 c_1 + b_1^2 c_0 - b_2 c_0) \right. \\ & \left. \left. + \frac{1}{3} (c_3 - b_1 c_2 + b_1^2 c_1 - b_2 c_1 - b_1^3 c_0 + 2 b_1 b_2 c_0 - b_3 c_0) \right] x^3 + \mathcal{O}(x^4) \right\}, \quad (12) \\ c_i \equiv \frac{\gamma_{m,i}^{(n_f)}}{\beta_0^{(n_f)}}, \quad b_i \equiv \frac{\beta_i^{(n_f)}}{\beta_0^{(n_f)}}. \end{aligned}$$

If $R(s)$ is evaluated at n -loop order, the curly bracket of Eq. (12) has to be evaluated up to, and including, the term $\propto x^{n-1}$.

The matching between $\bar{m}_Q^{(n_f)}$ and $\bar{m}_Q^{(n_f-1)}$ is determined through the equation

$$\bar{m}_Q^{(n_f-1)} = \zeta_m \bar{m}_Q^{(n_f)}, \quad (13)$$

where the function ζ_m can again be found in App. E.4. The procedure for the evaluation of $\bar{m}_Q^{(n_f)}(\mu)$ from the input $\bar{m}_Q(\bar{m}_Q)$ in `rhad` is called `rundecmass` (see App. D).

Note that the evaluation of $\bar{m}_Q^{(n_f)}(\mu)$ is only required if the user decides to use $\overline{\text{MS}}$ masses for the evaluation of $R(s)$. In this case, in `parameters.f` (see App. C),

```
lmsbar = .true.
```

and the values for `massc`, `massb`, `masst` have to be set to the scale invariant masses $\bar{m}_c(\bar{m}_c)$, $\bar{m}_b(\bar{m}_b)$, $\bar{m}_t(\bar{m}_t)$, respectively. If one chooses to use pole masses instead, one defines

```
lmsbar = .false.
```

and sets `massc`, `massb`, `masst` equal to the on-shell masses M_c , M_b , M_t , respectively. `rhad` will then simply use these values throughout the calculation.

There is one exception where we do *not* allow a choice between on-shell and $\overline{\text{MS}}$ mass: For “power-suppressed” corrections, *i.e.*, double-bubble diagrams that contain a heavy secondary quark loop (see Fig. 3 (e) with $m_2 \gg \sqrt{s}, m_1$), the heavy quark mass is *always* inserted in the on-shell scheme. If the input for the heavy mass is provided in the $\overline{\text{MS}}$ scheme, the corresponding on-shell value is evaluated within `rhad` by the subroutine `mms2mos` (see App. D), using the proper conversion relations [3, 4, 5].

3 Notation and tree-level result

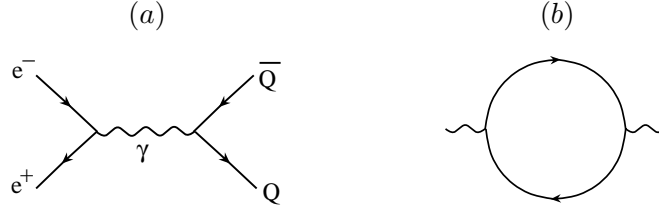


Figure 1: (a) Tree-level graph for $e^+e^- \rightarrow Q\bar{Q}$. (b) One-loop photon polarization function.

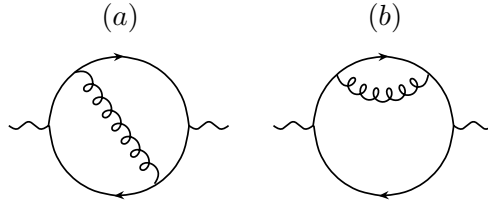


Figure 2: Diagrams contributing to $R(s)$ at one-loop level.

The tree level result for $R_Q(s)$ is part of every introductory course in quantum field theory. It reads

$$R_Q^{(0)}(s) = n_c \mathcal{V}_Q^2 r_V^{(0)}(s, m_Q), \quad \text{with} \quad r_V^{(0)}(s, M_Q) = \frac{v_Q}{2}(3 - v_Q^2), \quad (14)$$

where $n_c = 3$ is the number of colors, and \mathcal{V}_Q is the electric charge of the quark Q in units of the proton charge. *I.e.*,

$$\mathcal{V}_u = \mathcal{V}_c = \mathcal{V}_t = +\frac{2}{3}, \quad \mathcal{V}_d = \mathcal{V}_s = \mathcal{V}_b = -\frac{1}{3}. \quad (15)$$

v_Q denotes the quark velocity,

$$v_Q = \sqrt{1 - \frac{4M_Q^2}{s}}, \quad (16)$$

where \sqrt{s} is the c.m.s. energy. Note that we define v_Q in terms of the on-shell mass, M_Q (see Sect. 2). This becomes relevant at higher orders, where we refer to the definition of Eq. (16).

4 One-loop result

Sample diagrams that contribute to the one-loop approximation of $R(s)$ are shown in Fig. 2. Their imaginary part has been evaluated a long time ago in the context of QED [6]. In its most compact form, the result reads

$$R_Q^{(1)}(s) = n_c \mathcal{V}_Q^2 r_V^{(1)}(s, m_Q), \quad (17)$$

with

$$r_V^{(1)}(s, M_Q) = C_F \frac{3 - v_Q^2}{2} \left[(1 + v_Q^2) \left(\text{Li}_2(p^2) + 2\text{Li}_2(p) - \ln p \ln \frac{(1 + v_Q)^3}{8v_Q^2} \right) + 3v_Q \ln \frac{1 - v_Q^2}{4v_Q} - v_Q \ln v_Q + \frac{33 + 22v_Q^2 - 7v_Q^4}{8(3 - v_Q^2)} \ln \frac{1 + v_Q}{1 - v_Q} + \frac{15v_Q - 9v_Q^3}{4(3 - v_Q^2)} \right], \quad (18)$$

where $p = (1 - v_Q)/(1 + v_Q)$ and $C_F = 4/3$. In the limit $v_Q \rightarrow 1$, one obtains $r_V^{(1)} = 3C_F/4$ which, after taking into account the coupling and color factors, leads to the following expression for the QED corrections:

$$\delta R_Q^{\text{QED}} = n_c \mathcal{V}_Q^4 \frac{3}{4} \frac{\alpha}{\pi}. \quad (19)$$

The tree-level and one-loop functions and their correspondence in `rhad` are summarized in Tab. 1.

| notation | in <code>rhad</code> | diagrams |
|-------------|----------------------|------------|
| $r_V^{(0)}$ | <code>rv0</code> | Fig. 1 (b) |
| $r_V^{(1)}$ | <code>rv1</code> | Fig. 2 |

Table 1: Contributions to $R(s)$ at tree-level and one-loop order.

5 Two-loop result

Starting from two-loop order, a general analytic expression for $R(s)$ is no longer available. Typical diagrams are shown in Fig. 3. The full set can be obtained from these diagrams by attaching the two external photon lines to the quark lines at arbitrary points. Only certain classes of diagrams have been evaluated in closed form. Nevertheless, the analytic evaluation of different kinematical limits, combined with appropriate interpolation among these limits, have resulted in extremely accurate semi-analytical approximations to the full result. Thus, for all practical purposes, the full mass dependence is available at order α_s^2 .

Two main new features occur at the two-loop level that are absent at lower orders. First, there are contributions that are due to the non-Abelian character of QCD and have no correspondence in QED. These are diagrams with a three-gluon coupling (see Fig. 3 (c) and

(*d*); the four-gluon coupling occurs for the first time at three-loop order). The second new feature is that a second quark line can appear, with the effect that the result may depend on two different quark masses m_1 and m_2 (see Fig. 3 (*e*)).

It is clear that the simplest set of diagrams to evaluate are the ones with self-energy insertions in a gluon propagator, Fig. 3 (*d*), (*e*). In fact, the cases with massless insertions (*i.e.*, gluons and massless quarks) are known in closed analytical form, for general values of s and m_1 [7, 8]. The same is true for $m_1 = 0$, $m_2 \neq 0$ [9] (labels in accordance with Fig. 3 (*e*)). The case $m_1 = m_2$ is known in terms of a two-dimensional integral representation [7, 10]. For $m_1 \ll m_2$, the coefficient of the leading term in an expansion around $s/m_2^2 \rightarrow 0$ is known in closed form [11]. For $m_1 = 0$ [12], this term was shown to approximate the exact s/m_2^2 dependence [9] extremely well, even up to the threshold $s = 4m_2^2$.

The diagrams without self-energy insertions on gluon lines have not yet been evaluated in closed form for general values of m_Q and s . The massless limit has been known for quite some time [13]. Subsequently, mass corrections in the high energy limit have been computed: The m_Q^2/s terms can be obtained by a simple Taylor expansion of the integrand [14]; the m_Q^4/s^2 terms were derived from the $\overline{\text{MS}}$ operator product expansion of $\Pi(q^2)$, combined with renormalization group relations [15]; and the evaluation of the higher order terms (up to m_Q^{12}/s^6) was achieved by systematically expanding the Feynman integrals [16].

However, one should note that the convergence of such a high-energy expansion is not guaranteed below the highest threshold of the diagrams under consideration. For example, the non-planar diagram in Fig. 3 (*b*) has a four-quark cut at $q^2 = (4m_Q)^2$, meaning that the expansion around $m_Q^2/s \rightarrow 0$ formally converges only above $s = (4m_Q)^2$. Nevertheless, in practice one often observes also satisfactory convergence below the threshold [16].

A result that is valid in the full kinematic range was obtained in Ref. [17] (see also Ref. [18]). To this aim, the high-energy limit was combined with up to eight moments of the polarization function obtained through an expansion for $q^2 \rightarrow 0$. This information was combined with additional input from the threshold region around $q^2 = 4m_Q^2$, using a conformal mapping and Padé approximation in order to arrive at a three-loop expression for $\Pi(q^2)$. For all known practical applications, this approximate result is equivalent to an analytic expression for $\Pi(q^2)$ and, after taking the imaginary part, for $R(s)$.

Let us now explicitly parameterize the two-loop contribution to $R(s)$. We can write

$$R_Q^{(2)}(s) = n_c \mathcal{V}_Q^2 \left[r_V^{\text{F}}(s, m_Q) + r_V^{\text{A}}(s, m_Q) + \sum_q r_V^{\text{db}}(s, m_Q, m_q) \right], \quad (20)$$

where the sum runs over all quark flavors. $r_V^{\text{F}} \propto C_F^2$ denotes contributions from Abelian diagrams, $r_V^{\text{A}} \propto C_A C_F$ comes from non-planar and non-Abelian diagrams, and $r_V^{\text{db}} \propto C_F T$ (“double-bubble”) arises from diagrams with two separate quark lines. $C_F = 4/3$, $C_A = 3$ and $T = 1/2$ are color factors of QCD. For later reference, it is convenient to introduce additional functions that refer to specific limits of r_V^{db} :

$$r_V^{\text{db}}(s, m_Q, 0) \equiv r_V^{\text{L}}(s, m_Q), \quad r_V^{\text{db}}(s, m_Q, m_Q) \equiv r_V^{\text{T}}(s, m_Q). \quad (21)$$

See also Tab. 2 for more details. Note that r_V^{db} introduces contributions from secondary quarks q other than Q , both virtual and real. They arise through the splitting of gluons into a quark–anti-quark pair.

In the massless case, one has the simple expressions

$$\begin{aligned}
r_V^F(s, m_Q = 0) &= C_F^2 \left(-\frac{3}{32} \right), \\
r_V^A(s, m_Q = 0) &= C_A C_F \left(\frac{123}{32} - \frac{11}{4} \zeta_3 - \frac{11}{16} L_{s\mu} \right), \\
r_V^{\text{db}}(s, m_1 = 0, m_2 = 0) &= C_F T \left(-\frac{11}{8} + \zeta_3 + \frac{1}{4} L_{s\mu} \right).
\end{aligned} \tag{22}$$

where $L_{s\mu} \equiv \ln(s/\mu^2)$ and $\zeta_3 \approx 1.20206$. The expressions in the massive case are given in App. E.1.

In the following, the expressions adopted for the individual contributions are described, and their origin is given.

- For $r_V^F(s, m_Q)$ and $r_V^A(s, m_Q)$ we use the full mass dependence as given by the Padé results of Eqs. (36), (39) [17].
- For the double-bubble contribution $r_V^{\text{db}}(s, m_1, m_2)$, we have to distinguish several cases:
 - $m_1 = m_2 = m_Q$: For $\sqrt{s} \leq 4m_Q$, we use the analytic formula as given in Eq. (44) [7]. For $\sqrt{s} > 4m_Q$, the full mass dependence is known in terms of a two-fold integral representation, see Eq. (46) [7]. For the sake of speed, however, we use the high energy expansion of Eq. (48) [16]. Numerical differences to the integral representation are completely negligible. Nevertheless, the user may switch to the integral formula by setting `lrvctexp = .false.` in `rhad`.
 - $m_2 < m_1$: We apply an expansion for $m_2^2 \ll m_1^2 (< s/4)$:
 1. At $\mathcal{O}(m_2^0)$, the full m_1 -dependence is used in the form of the analytic result of Eq. (41) (for $x = L$) [7].
 2. At $\mathcal{O}(m_2^2)$, we neglect the m_1 dependence. It turns out that this contribution vanishes which can be seen in Eq. (52).
 3. Higher orders in m_2 are neglected.
 - $(2m_1)^2 < s < (2m_2)^2$: If $m_1 = 0$, we use the analytical result of Eq. (49) [9], including the full dependence on m_2 . If $m_1 \neq 0$, we use the leading term in $1/m_2^2$, keeping its full m_1^2 dependence, see Eq. (54). This expression has been obtained in Ref. [11].
 - $(2m_1)^2 < (2m_2)^2 < s$: If $m_1 = 0$, we use the analytical result of Eq. (49) [9], including the full dependence on m_2 . If $m_1 \neq 0$, we apply an expansion in the limit $m_1^2 \ll m_2^2 (< s/4)$:
 1. At $\mathcal{O}(m_1^0)$, we use the analytical result of Eq. (49) [9] for the full m_2 dependence.
 2. At $\mathcal{O}(m_1^2)$, we neglect all effects from non-zero m_2 . The corresponding expression for $r_V^{\text{db}}(s, m_1, 0)$ is given in Eq. (53).
 3. Higher orders in m_1 are neglected.

Note that we set the ratios m_c^2/m_t^2 and m_b^2/m_t^2 to zero and consider mass corrections due to the presence of an additional light quark only for c -quark effects in b -quark production.

For the sake of completeness, let us remark that also the two-loop corrections of order $\alpha\alpha_s$ and order α^2 for massless quarks [19] are known. Numerically, these contributions are very small. Nevertheless, we include the mixed corrections of order $\alpha\alpha_s$ into `rhad`, which modifies Eq. (19) to

$$\delta R_Q^{\text{QED}} = n_c \mathcal{V}_Q^4 \frac{3\alpha}{4\pi} \left(1 - \frac{1}{3} \frac{\alpha_s(\mu)}{\pi} \right). \quad (23)$$

Higher order QED or mixed QED/QCD effects are numerically irrelevant and will be neglected [20].

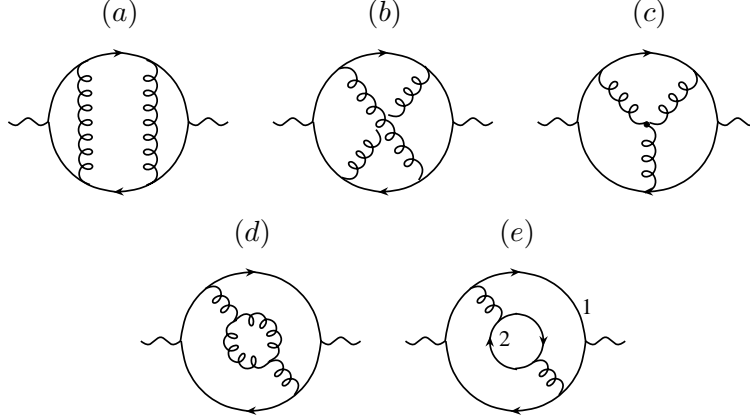


Figure 3: Classes of diagrams contributing to $R(s)$ at two-loop level. (For the issue of counting loops, see the discussion at the end of Sect. 1.)

| notation | in rhad | diagrams | m_1 | m_2 |
|-------------------|---------|---------------|-------|-------|
| r_V^F | rvcf | (a), (b) | m_Q | – |
| r_V^A | rvca | (b), (c), (d) | m_Q | – |
| r_V^{db} | rvdb | (e) | m_1 | m_2 |
| r_V^L | rvnl | (e) | m_Q | 0 |
| r_V^T | rvct | (e) | m_Q | m_Q |

Table 2: Different contributions to $R(s)$ at two-loop order. The column “diagrams” refers to Fig. 3, where a sample diagram is shown for each class.

6 Three-loop result

At order α_s^3 , a new class of diagrams contributes to R_{had} , the so-called “singlet diagrams.” They differ from the non-singlet diagrams in the sense that, in the singlet case, the external currents are not connected by a common quark line. A typical diagram is shown in Fig. 4(d). The non-singlet diagrams (see Fig. 4(a)–(c)) are numerically dominant, but `rhad` includes both contributions. We will describe them in more detail in what follows.

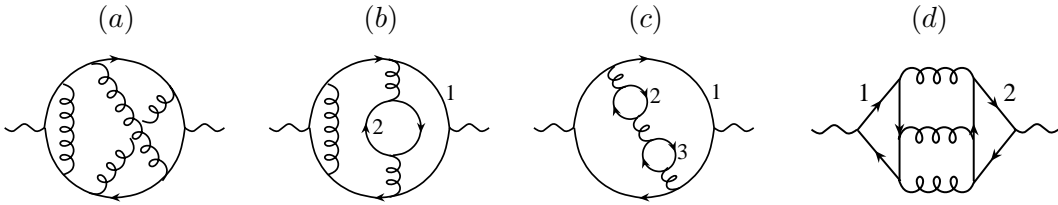


Figure 4: Classes of diagrams contributing to $R(s)$ at three-loop level.

| notation | in rhad | diagrams | m_1 | m_2 | m_3 |
|---------------------------|----------|---------------|-------|------------|------------|
| $r_V^{(3)}$ | rv3 | (a), (b), (c) | m_Q | m_Q or 0 | m_Q or 0 |
| $\delta r_0^{(3)}$ | deltar03 | (b), (c) | 0 | m_Q | m_Q or 0 |
| $r_{V,\text{sing}}^{(3)}$ | rv3sing | (d) | m_1 | m_2 | – |

Table 3: Different contributions to $R(s)$ at three-loop order (as far as available). The column “diagrams” refers to Fig. 4, where a sample diagram is shown for each contribution.

6.1 Non-singlet contributions

The knowledge of $R(s)$ at three-loop level is restricted to the high energy limit. The massless limit was obtained for the first time in Ref. [21] and later confirmed through an independent calculation in Ref. [22].

Mass corrections are known up to $\mathcal{O}(m_Q^4/s^2)$: The quadratic terms were obtained from renormalization group identities [23], while the quartic mass terms were evaluated by applying the methods of Ref. [15] at three-loop level [24].

Let us briefly discuss how we treat mass effects from massive inner quark loops. At three-loop level, there can be three different quark types in one diagram, with, say $m_1 > m_2 > m_3$. The approximation that we apply is to take all terms including m_1^4 and m_2^2 , neglecting mixed terms of order $m_1^2 m_2^2$. Mass effects from m_3 are also neglected. In addition, we do not consider power-suppressed terms, *i.e.* diagrams that contain a quark q with $s < s_q^{\text{thr}}$.

With these approximations in mind, we can write the three-loop contribution as

$$R_Q^{(3)}(s) = n_c \mathcal{V}_Q^2 \left[r_V^{(3)}(s, m_Q, n_f) + \sum_{q \neq Q} \delta r_0^{(3)}(s, m_q, n_f) \right]. \quad (24)$$

$\delta r_0^{(3)}(s, m_q, n_f)$ denotes the mass corrections due to massive inner quark loops different from Q . According to the approximations above, it vanishes for $s < s_q^{\text{thr}}$ and also for $m_q = 0$.

Note that n_f itself depends on the c.m.s. energy. Assume, for example, that $s < s_c^{\text{thr}}$. Then we have $n_f = 3$ and

$$R_Q^{(3)}(s) = n_c \mathcal{V}_Q^2 r_V^{(3)}(s, 0, 3), \quad Q = u, d, s. \quad (25)$$

For $s_c^{\text{thr}} < s < s_b^{\text{thr}}$, we have $n_f = 4$ and thus the non-zero contributions are

$$R_Q^{(3)}(s) = n_c \mathcal{V}_Q^2 \left[r_V^{(3)}(s, 0, 4) + \delta r_0^{(3)}(s, m_c, 4) \right], \quad Q = u, d, s, \quad (26)$$

and $R_c^{(3)}(s) = n_c \mathcal{V}_c^2 r_V^{(3)}(s, m_c, 4)$.

For $s_b^{\text{thr}} < s < s_t^{\text{thr}}$, it is $n_f = 5$ and

$$R_Q^{(3)}(s) = n_c \mathcal{V}_Q^2 \left[r_V^{(3)}(s, 0, 5) + \delta r_0^{(3)}(s, m_c, 5) + \delta r_0^{(3)}(s, m_b, 5) \right], \quad Q = u, d, s,$$

$$R_c^{(3)}(s) = n_c \mathcal{V}_c^2 \left[r_V^{(3)}(s, m_c, 5) + \delta r_0^{(3)}(s, m_b, 5) \right], \quad (27)$$

$$R_b^{(3)}(s) = n_c \mathcal{V}_b^2 \left[r_V^{(3)}(s, m_b, 5) + \delta r_0^{(3)}(s, m_c, 5) \right].$$

Finally, for $s > s_t^{\text{thr}}$, all masses except for m_t are neglected, and, with $n_f = 6$, we have

$$R_Q^{(3)}(s) = n_c \mathcal{V}_Q^2 \left[r_V^{(3)}(s, 0, 6) + \delta r_0^{(3)}(s, m_t, 6) \right], \quad Q = u, d, c, s, b, \quad (28)$$

$$R_t^{(3)}(s) = n_c \mathcal{V}_t^2 r_V^{(3)}(s, m_t, 6).$$

As mentioned before, in Eq. (27) it is understood that all c -quark mass effects are included only at $\mathcal{O}(m_c^2)$.

The expressions for $r_V^{(3)}(s, m_Q, n_f)$ and $\delta r_0^{(3)}(s, m_Q, n_f)$ are listed in App. E.2.

6.2 Singlet contributions

As already mentioned above, singlet diagrams are characterized by the fact that each of the external photons couples to a separate quark line (see, *e.g.*, Fig. 4 (*d*)). The singlet contribution arises first at three-loop level; at two-loop level, where the two quark lines are connected by only two gluons, it is zero due to Furry's theorem.

We write the singlet contribution to $R(s)$ in the following way:

$$R_{\text{sing}}(s) = n_c \sum_{q, q'} \mathcal{V}_q \mathcal{V}_{q'} r_{V, \text{sing}}^{(3)}(s, m_q, m_{q'}), \quad (29)$$

where the sum over q and q' runs over all active quark flavors. *E.g.*, for $\sqrt{s} = 12$ GeV it includes all quarks except for the top quark. Again, only the high energy expansion is known. Quadratic mass terms are absent, and the expression including quartic mass terms reads:

$$r_{V, \text{sing}}^{(3)}(s, m_1, m_2) = \frac{55}{216} - \frac{5}{9} \zeta_3 + \frac{m_1^4}{s^2} \left(-\frac{10}{9} + \frac{25}{3} \zeta_3 \right) + \frac{m_2^4}{s^2} \left(-\frac{10}{9} + \frac{25}{3} \zeta_3 \right). \quad (30)$$

Note that, if $m_1 \neq m_2$, we neglect the lighter of the two masses. Since this is the lowest order where singlet terms occur, Eq. (30) is the same in the $\overline{\text{MS}}$ and in the on-shell mass scheme.

7 Four-loop result

The knowledge of the four-loop contribution to $R(s)$ is very limited. Only contributions of diagrams with two and three quark-loop insertions have been calculated. Sample diagrams are shown in Fig. 5 (c) and (d). The mass effects are evaluated up to order m_Q^2/s , so that the results are strictly only valid in the high-energy limit.

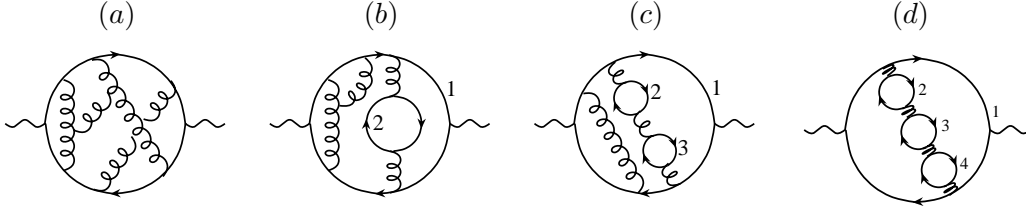


Figure 5: Classes of diagrams contributing to $R(s)$ at four-loop level.

We write the four-loop contribution as

$$\bar{R}_Q^{(4)}(s) = n_c \mathcal{V}_Q^2 \bar{r}_V^{(4)}(s, m_Q), \quad (31)$$

with

$$\begin{aligned} \bar{r}_V^{(4)}(s, m_Q) &= \bar{r}_0^{(4),0L}(s) + n_f \bar{r}_0^{(4),1L}(s) + n_f^2 r_0^{(4),2L}(s) + n_f^3 r_0^{(4),3L}(s) \\ &+ \frac{m_Q^2}{s} \left(\bar{r}_{V,2}^{(4),0L}(s) + n_f \bar{r}_{V,2}^{(4),1L}(s) + n_f^2 r_{V,2}^{(4),2L}(s) + n_f^3 r_{V,2}^{(4),3L}(s) \right), \end{aligned} \quad (32)$$

where the bar indicates that the expressions are estimates rather than approximations or even exact results. n_f is the number of active flavors, varying with the c.m.s. energy as discussed in Sect. 2.

$r_0^{(4),3L}$ is the renormalon-type contribution with three massless quark insertions on the gluon propagator, see Fig. 5 (d). It has been evaluated in Ref. [25], where the general structure of the terms of order $\alpha_s(\alpha_s n_f)^n$ was derived. Recently, the analytic expression for $r_0^{(4),2L}$ became available [26]. It required the evaluation of massless four-loop two-point functions in combination with the method of Ref. [22] (see also Ref. [18]) to derive the imaginary part of the five-loop contributions as shown in Fig. 5 (c). The same method has been used in combination with the technique derived in Ref. [23] for the computation of the quadratic mass corrections $r_{V,2}^{(4),2L}$ and $r_{V,2}^{(4),3L}$ [27].

Estimates for the full massless four-loop result have been known before and are still a subject of interest [28, 29, 30]. We determine $\bar{r}_0^{(4)}(s)$ and $\bar{r}_0^{(4),L}(s)$ by subtracting the known n_f^2 and n_f^3 contributions from the estimates of Ref. [28] at $n_f = 1, \dots, 6$, and fitting the resulting six “data points” by a linear function in n_f . One finds, for $\mu^2 = s$,

$$\begin{aligned} \bar{r}_0^{(4),0L}(s) &= -1.86 \cdot 10^2, & \bar{r}_0^{(4),1L}(s) &= 21.3, \\ r_0^{(4),2L}(s) &= -7.97 \cdot 10^{-1}, & r_0^{(4),3L}(s) &= 2.15 \cdot 10^{-2}. \end{aligned} \quad (33)$$

The logarithmic contributions follow from the lower order terms through renormalization group invariance and are collected in App. E.3. Once the exact results for $r_0^{(4),0L}$ and $r_0^{(4),1L}$ become available, the approximate ones can easily be replaced in **rhad**.

Using the same method for the quadratic mass terms in combination with the estimates of Ref. [27] we obtain, in the $\overline{\text{MS}}$ scheme

$$\begin{aligned} \bar{r}_{V,2}^{(4),0L}(s) &= 7.11 \cdot 10^3, & \bar{r}_{V,2}^{(4),1L}(s) &= -1.43 \cdot 10^3, \\ r_{V,2}^{(4),2L}(s) &= 49.1, & r_{V,2}^{(4),3L}(s) &= -0.204. \end{aligned} \tag{34}$$

In App. E.3, the corresponding result for on-shell quark masses is listed together with the logarithmic contributions.

For completeness, the function implemented in `rhad` is listed in Tab.4. Note that at $\mathcal{O}(\alpha_s^4)$, the corrections analogous to $\delta r_0^{(3)}$ are neglected.

| notation | in rhad |
|-------------|---------|
| $r_V^{(4)}$ | rv4 |

Table 4: Contribution to $R(s)$ at four-loop order.

8 Evaluating $R(s)$

In this section we describe how `rhad` evaluates $R(s)$ in the individual energy regions. Let us first recall that s_Q^{thr} defines the lowest value of the c.m.s. energy squared, s , at which the perturbative treatment of $Q\bar{Q}$ production is allowed; $R_Q(s)$ is defined to be zero for $s < s_Q^{\text{thr}}$. The *physical* threshold for $Q\bar{Q}$ production is at s_Q^{low} ; the user is advised, however, to disregard the results of `rhad` in the region between s_Q^{low} and s_Q^{thr} ($Q = c, b, t$).

The evaluation of the number of active flavors n_f , the strong coupling constant $\alpha_s^{(n_f)}(\mu)$, and, if required, the $\overline{\text{MS}}$ quark masses $\bar{m}_Q^{(n_f)}(\mu)$, from the input values s , μ , $\alpha_s^{(5)}(M_Z)$, and $\bar{m}_Q(\bar{m}_Q)$, has been described in Sect. 2. Let us now look in more detail at the specific contributions that enter $R(s)$ at certain values of s .

For $s < s_c^{\text{low}}$, *i.e.*, below the production threshold for two D_0 mesons, we have $n_f = 3$. The charm, bottom and top quark masses are decoupled and thus their contribution goes like $\alpha_s^2 s/m_q^2$ ($q = c, b, t$), see Eqs. (49,54). All other correction terms are evaluated in the massless limit.

In the region $s_c^{\text{thr}} < s < s_b^{\text{low}}$ one has $n_f = 4$. $\alpha_s^{(4)}(\mu)$ is evaluated from the input $\alpha_s^{(5)}(M_Z)$, and, in the $\overline{\text{MS}}$ mass scheme, $\bar{m}_c^{(4)}(\mu)$ is obtained from the input quantity $\bar{m}_c(\bar{m}_c)$ (see Sect. 2). In the on-shell mass scheme, the input value M_c is used unchanged throughout the calculation. The full charm quark mass dependence (inasmuch it is known) is taken into account. Bottom and top quark are decoupled and enter through the power-suppressed terms, Eqs. (49,54), at order α_s^2 .

At c.m.s. energies above s_b^{thr} and below s_t^{low} , the situation is similar to the previously described region, but with $n_f = 5$. Note, however, that in the $\overline{\text{MS}}$ scheme not only $\bar{m}_b^{(5)}(\mu)$ is needed for the numerical evaluation, but also $\bar{m}_c^{(5)}(\mu)$. It is obtained from the input $\bar{m}_c(\bar{m}_c)$ using the routine `rundecmass` (see Sect. D).

| $\sqrt{s} = 2 \text{ GeV}$ | | | $\sqrt{s} = 5 \text{ GeV}$ | | | |
|----------------------------|------------|--------|----------------------------|------------|----------|--------|
| order | α_s | $R(s)$ | order | α_s | $R_c(s)$ | $R(s)$ |
| 0 | 0.1180 | 2.0012 | 0 | 0.1180 | 1.2199 | 3.2220 |
| 1 | 0.2726 | 2.1747 | 1 | 0.2025 | 1.4956 | 3.6267 |
| 2 | 0.2981 | 2.2223 | 2 | 0.2120 | 1.5950 | 3.7467 |
| 3 | 0.2984 | 2.2049 | 3 | 0.2123 | 1.5825 | 3.7272 |
| 4 | 0.2973 | 2.1835 | 4 | 0.2122 | 1.5467 | 3.6867 |

Table 5: Hadronic R -ratio at $\sqrt{s} = 2 \text{ GeV}$ ($n_f = 3$, left) and $\sqrt{s} = 5 \text{ GeV}$ ($n_f = 4$, right). Note the change in α_s which is consistently evaluated from $\alpha_s^{(5)}(M_Z)$. The parameter settings are given in App. C.2.

| $\sqrt{s} = 12 \text{ GeV}$ | | | | |
|-----------------------------|------------|----------|----------|--------|
| order | α_s | $R_c(s)$ | $R_b(s)$ | $R(s)$ |
| 0 | 0.1180 | 1.3304 | 0.2675 | 3.6001 |
| 1 | 0.1667 | 1.4199 | 0.3496 | 3.8778 |
| 2 | 0.1706 | 1.4269 | 0.3803 | 3.9265 |
| 3 | 0.1709 | 1.4198 | 0.3797 | 3.9148 |
| 4 | 0.1709 | 1.4158 | 0.3756 | 3.9050 |

Table 6: Hadronic R -ratio at $\sqrt{s} = 12 \text{ GeV}$ ($n_f = 5$).

For $s > s_t^{\text{thr}}$, $\alpha_s^{(6)}(\mu)$ and $\bar{m}_t^{(6)}(\mu)$ are needed for the evaluation of $R(s)$. At these energies, no mass corrections from lighter quarks are considered.

Tab. 5 and 6 show the results for $R(s)$ with the default settings (see Sect. C), for different values of the c.m.s. energy. The individual rows correspond the different orders of perturbation theory. In the case of $\sqrt{s} = 5 \text{ GeV}$ and $\sqrt{s} = 12 \text{ GeV}$, we also show the partial contributions to $R(s)$ arising from massive quarks. The second column contains the value of $\alpha_s^{(n_f)}(\sqrt{s})$, with the appropriate n_f .

Tab. 7 contains the results for $\alpha_s(s)$, $R(s)$, $R_c(s)$ and $R_b(s)$ for the energy region between $\sqrt{s} = 1.8 \text{ GeV}$ and $\sqrt{s} = 20 \text{ GeV}$, sparing out those parts where perturbation theory is not applicable. We adopted the default values of `rhad` given in App. C with `iord = 4`. In Fig. 6 the data for $R(s)$ (full curve) are shown in graphical form. The shaded bands mark the uncertainty of $R(s)$ induced by the variation of $\alpha_s(M_Z)$, μ , M_c and M_b in the range

$$\begin{aligned}
\alpha_s(M_Z) &= 0.118 \pm 0.003, \\
M_c &= (1.65 \pm 0.15) \text{ GeV}, \\
M_b &= (4.75 \pm 0.2) \text{ GeV}, \\
\mu &\in \left[\frac{\sqrt{s}}{2}, 2\sqrt{s} \right].
\end{aligned} \tag{35}$$

| \sqrt{s} (GeV) | $\alpha_s(s)$ | $R_c(s)$ | $R_b(s)$ | $R(s)$ |
|------------------|---------------|----------|----------|--------|
| 1.80 | 0.3148 | 0.0000 | 0.0000 | 2.1895 |
| 2.20 | 0.2833 | 0.0000 | 0.0000 | 2.1780 |
| 2.60 | 0.2620 | 0.0000 | 0.0000 | 2.1684 |
| 3.00 | 0.2463 | 0.0000 | 0.0000 | 2.1607 |
| 3.40 | 0.2342 | 0.0000 | 0.0000 | 2.1544 |
| 3.73 | 0.2260 | 0.0000 | 0.0000 | 2.1499 |
| 4.80 | 0.2150 | 1.5681 | 0.0000 | 3.7097 |
| 5.00 | 0.2122 | 1.5467 | 0.0000 | 3.6867 |
| 6.00 | 0.2007 | 1.4842 | 0.0000 | 3.6174 |
| 7.00 | 0.1919 | 1.4556 | 0.0000 | 3.5836 |
| 8.00 | 0.1850 | 1.4399 | 0.0000 | 3.5637 |
| 9.00 | 0.1793 | 1.4301 | 0.0000 | 3.5505 |
| 10.00 | 0.1744 | 1.4235 | 0.0000 | 3.5410 |
| 10.52 | 0.1722 | 1.4209 | 0.0000 | 3.5371 |
| 11.20 | 0.1736 | 1.4186 | 0.3793 | 3.9133 |
| 12.00 | 0.1709 | 1.4158 | 0.3756 | 3.9050 |
| 13.00 | 0.1679 | 1.4129 | 0.3717 | 3.8964 |
| 14.00 | 0.1652 | 1.4106 | 0.3685 | 3.8891 |
| 15.00 | 0.1628 | 1.4087 | 0.3659 | 3.8830 |
| 16.00 | 0.1606 | 1.4070 | 0.3636 | 3.8778 |
| 17.00 | 0.1586 | 1.4056 | 0.3618 | 3.8732 |
| 18.00 | 0.1567 | 1.4044 | 0.3602 | 3.8692 |
| 19.00 | 0.1550 | 1.4033 | 0.3589 | 3.8657 |
| 20.00 | 0.1534 | 1.4023 | 0.3577 | 3.8626 |

Table 7: $\alpha_s(s)$, $R_c(s)$, $R_b(s)$, and $R(s)$ for various values of s .

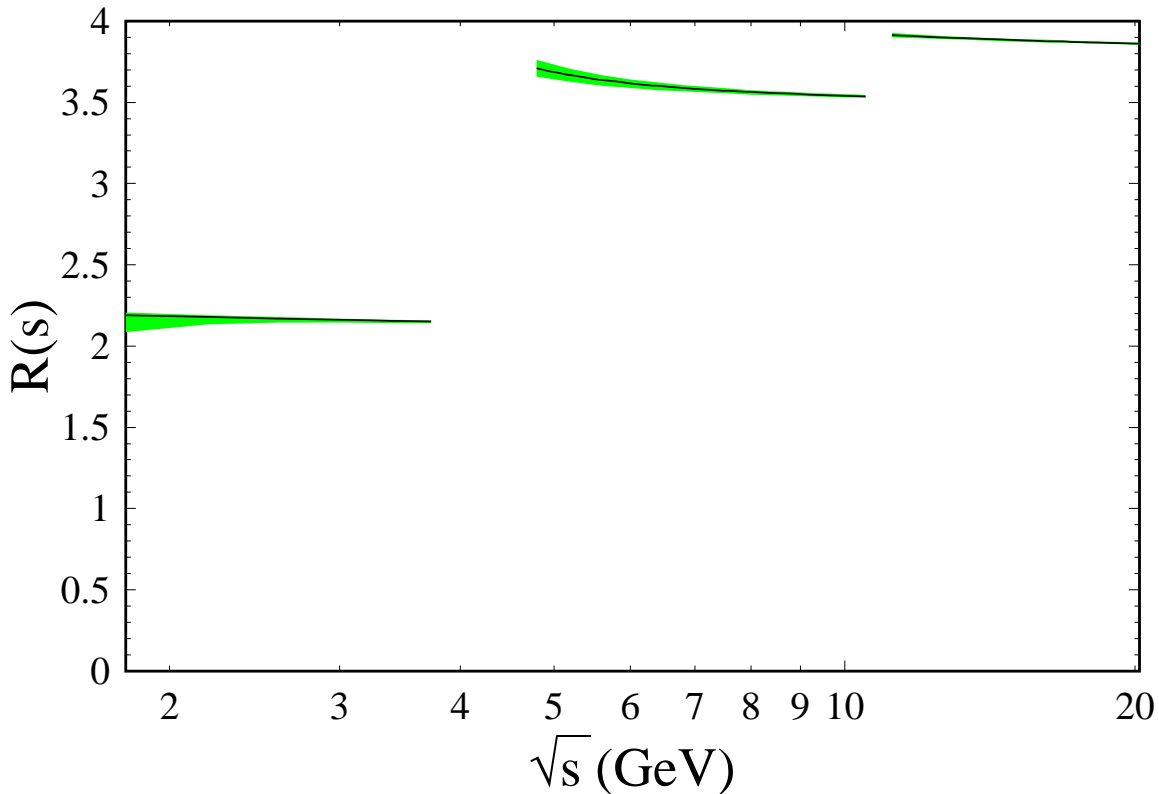


Figure 6: $R(s)$ for $1.8 \text{ GeV} < \sqrt{s} < 20 \text{ GeV}$. The central curve (solid line) is obtained using the default values specified in App. C and corresponds to the results given in Tab. 7. The error bands are obtained by varying $\alpha_s(M_Z)$, μ , M_c and M_b within the limits of Eq. (35). Not shown are the perturbatively inaccessible regions between s_Q^{low} and s_Q^{thr} ($Q = c, b$, see Sect. 1).

9 A typical program

It is instructive to look at a typical program that evaluates $R(s)$. We set the c.m.s. energy to $\sqrt{s} = 12 \text{ GeV}$, and split the result according to the contributions from the individual quarks. The occurring functions will be described in more detail in App.B, but their functionality should be clear from the following program.

Input. The corresponding `fortran` program would look as follows.

```

program example

implicit real*8(a-h,m-z)
implicit integer(i,j)
implicit character*60(k)
implicit logical(l)

include 'common.f'

```

```

sqrt(s) = 12.d0
scms = sqrt(s)*sqrt(s)

call parameters(scms)
call init(scms)

rall = rhad(scms)
ru = ruqrk(scms)
rd = rdqrk(scms)
rs = rsqrk(scms)
rc = rcqrk(scms)
rb = rbqrk(scms)
rt = rtqrk(scms)
rsg = rsinglet(scms)
rem = rqed(scms)

print*, 'R_had = ',rall
print*, 'R_u = ',ru
print*, 'R_d = ',rd
print*, 'R_s = ',rs
print*, 'R_c = ',rc
print*, 'R_b = ',rb
print*, 'R_t = ',rt
print*, 'R_sing = ',rsg
print*, 'R_QED = ',rem

end

```

Output. If lverbose is set to .true. the output reads:

```

          rhad.f -- Version 1.00
by Robert Harlander and Matthias Steinhauser
          December 2002

```

Order of calculation: 4

Scales:

```

sqrt(s) = 12.000 GeV
mu       = 12.000 GeV
thrc    = 4.800 GeV
thrb    = 11.200 GeV
thrt    = 360.000 GeV

```

Number of active flavors:

```

nf = 5

```

Coupling constants:

```
alpha_QED    = 1 / ( 137.036 )
alpha_s(Mz)  = 0.1180           [ Mz = 91.1876 GeV ]
alpha_s(mu)  = 0.1709360043
```

Quark masses:

```
M_c         = 1.65 GeV
M_b         = 4.75 GeV
M_t         = 175.00 GeV
```

General switches (F=False, T=True):

```
only massless terms      : F
power suppressed terms   : T
QED corrections          : T
singlet contributions    : T
alphas^3 m^2 included   : T
alphas^3 m^4 included   : T
alphas^4 m^2 included   : T
-- end of parameters --
R_had = 3.9049832
R_u   = 1.40765446
R_d   = 0.351913615
R_s   = 0.351913615
R_c   = 1.41577367
R_b   = 0.375554797
R_t   = 0.
R_sing = -4.42977631E-05
R_QED = 0.00221733842
```

If `lverbose = .false.`, only the lines after “`-- end of parameters --`” are printed. The parameter list displays the most important initializations, like the value of $\alpha_s^{(5)}(M_Z)$ and the renormalization scale μ . It also contains values for parameters that were derived from these settings, like the number of active flavors n_f , and the strong coupling constant $\alpha_s^{(n_f)}(\mu)$.

10 Conclusions

In this paper we have discussed the perturbative corrections to the inclusive cross section $\sigma(e^+e^- \rightarrow \text{hadrons})$ and collected the analytical and semi-analytical formulas. This includes the full mass dependence up to order α_s^2 , the expansion up to quartic mass terms at order α_s^3 and the quadratic mass corrections at order α_s^4 . Furthermore, the running and decoupling formalism necessary for a consistent evaluation of the strong coupling constant and the $\overline{\text{MS}}$ quark masses has been presented.

The main subject of this paper, however, is a description of the `fortran` program `rhad` which allows for the evaluation of $R(s)$, including all currently available radiative corrections. The program is straightforward to use, in particular if the default parameter set

is adopted. Variations of the physical input values should be done such that they still resemble the physical case. The modularity of `rhad` allows for a simple extension once new corrections to the theoretical predictions for $R(s)$ become available. In conclusion, `rhad` can easily be used to compute, for example, the perturbative parts of the hadronic contributions to the running of the electromagnetic coupling, and the anomalous magnetic moment of the muon.

Acknowledgments

First of all, we are indebted to Hans Kühn for suggesting this project and for his valuable advice at all stages of its development. It is a pleasure to thank Thomas Teubner for his help and patience in debugging `rhad`. The comparison to his private code was an essential ingredient for the completion of this work. Furthermore, we thank him and Marek Jeżabek for providing `fortran` routines which have been used in preliminary versions of `rhad`. Thorsten Seidensticker kindly allowed us to include the unpublished analytical results of $r_V^{\text{db}}(s, m_1, m_2)$ in the limit $(2m_1)^2 < s < (2m_2)^2$. Furthermore, we thank the authors of Refs. [27, 30] for making the manuscripts accessible to us before publication.

Appendix

A Installation

The distribution of `rhad` contains the following files:

```
Examples  example.f  makefile      r012.f  rhad.f  vegas-rhad.f
common.f  funcs.f    parameters.f  r34.f   runal.f
```

`Examples` is a directory that contains programs to reproduce Tables 5, 6, and 7 of this paper. One example program is kept in the main directory, `example.f`. Its listing is shown in Sect. 9. It can be compiled by simply calling GNU make:

```
> gmake prog=example
```

The executable is named `xexample`.

If GNU make is not available, the `fortran` files can be compiled individually using

```
f77 -c -o <file>.o <file>.f
```

and then linked using

```
f77 -o xexample *.o
```

B Basic functions of `rhad`

Unless indicated otherwise, we use the following implicit type specifications in `rhad`:

```

IMPLICIT REAL*8(A-H,M-Z)
IMPLICIT INTEGER(I,J)
IMPLICIT CHARACTER*60(K)
IMPLICIT LOGICAL(L)

```

The functions that encode the different loop orders to $R(s)$ have already been discussed in Sects. 3–7, and in particular in Tables 1–4.

The proper sums of these contributions are taken by the following functions corresponding to $R_Q(s)$, $R_{\text{sing}}(s)$ and $\delta R_Q^{\text{QED}}(s)$ (photon exchange only):

```

rdqrk(s), ruqrk(s), rsqrk(s), rcqrk(s), rbqrk(s), rtqrk(s):
    R_d(s), R_u(s), R_s(s), R_c(s), R_b(s), R_t(s)

```

```

rsinglet(s): R_sing(s)

```

```

rqed(s):  $\sum_Q \delta R_Q^{\text{QED}}(s)$ 

```

The full R -ratio is obtained by calling `rhad(s)`, which adds the contributions from the individual quarks, depending on the c.m.s. energy.

The general structure of a `fortran` program from which the above functions are called is as follows:

```

program <name of program>
  <declaration of variables>
  <definition of s, e.g.:>
  include 'common.f'
  scms = 11.5d0**2
  call parameters(scms)
  call init(scms)
  <call of function to compute R(s)>
end

```

It is important to call the subroutines `parameters` and `init` (in this order), which define the parameters and evaluate $\alpha_s(\mu)$ and, if required, evolve and convert the masses. An explicit example program has been given in Sect. 9.

C The subroutine parameters

C.1 Description of the parameters

The file `parameters.f` contains the subroutine `parameters` and collects the most important variables that can be adjusted by the user. `parameters.f` should be understood as the input file for `rhad`. In Appendix C.2, our default settings are listed. Let us stress that, although many of the implemented formulas are valid over a large parameter range, one should vary the input parameters only within a sensible region about their default values. Unreasonable settings, like inverted mass hierarchies or the like, may lead to inconsistent results.

The following list describes the variables defined in `parameters.f`:

`lverbose`: Print values of parameters (see Sect. 8)

`iunit`: Output unit for parameter list.

`iord`: Order of the calculation. Values: `iord=0` (Born) to `iord=4`. It also governs the order at which the running coupling and the $\overline{\text{MS}}$ masses are evaluated.

`alphasmz`: $\alpha_s^{(5)}(M_Z)$. Input value for the strong coupling constant (see Sect. 2).

`lmsbar`: If `.true.`, evaluate $R(s)$ by using $\overline{\text{MS}}$ masses (see Sect. 2).

`massc`, `massb`, `masst`: Initial values for m_c , m_b , m_t . If `lmsbar = .true.`: scale invariant mass $\bar{m}_q(\bar{m}_q)$; otherwise: on-shell mass M_q (see Sect. 2).

`mu`: Renormalization scale μ at which α_s , the $\overline{\text{MS}}$ quark masses and $R(s)$ are evaluated (see Sect. 2).

`muc`, `mub`, `mut`: μ_c , μ_b , μ_t . Matching scales for the decoupling of the heavy quarks (see Sect. 2).

`lqed`: If `.true.`, include the lowest order QED and, if `iord.ge.2`, the mixed QED/QCD corrections (see Eqs. (19) and (23)).

`lmassless`: If `.true.`, neglect all quark masses.

`lpsup`: If `.true.`, include power-suppressed terms (see Eqs. (51),(54)).

`1a3m2`: If `.true.`, include $\alpha_s^3 m_Q^2$ terms (see Sect. E.2).

`1a3m4`: If `.true.`, include $\alpha_s^3 m_Q^4$ terms (see Sect. E.2).

`1a3sing`: If `.true.`, include singlet terms (see Sect. 6.2).

`1a4m2`: If `.true.`, include $\alpha_s^4 m_Q^2$ terms (see Sect. 7).

`thrc`, `thrb`, `thrt`: s_c^{thr} , s_b^{thr} , s_t^{thr} (see Sect. 1 and 8).

Thresholds for open (perturbative) c -, b -, and t -quark pair production.

`thrclow`, `thrblow`, `thrtlow`: s_c^{low} , s_b^{low} , s_t^{low} (see Sect. 1 and 8).

Perturbation theory is not applicable for $s_Q^{\text{low}} \leq s \leq s_Q^{\text{thr}}$, $Q \in \{c, b, t\}$. Note that these three parameters have no influence on the results; their only task is to remind the user of the problematic energy regions in the perturbative approach.

`sqmin`: minimal allowed value for the c.m.s. energy (see Sect. 1).

Note that not all parameters are independent: for example, if `lmassless = .true.`, `1a3m2`, `1a3m4`, and `1a4m2` will automatically be set to `.false.`

C.2 Default settings

The default settings in `parameters.f` are as follows:

```
      subroutine parameters(scms)
c..
c..  User-defined parameters.
c..
      implicit real*8(a-h,m-z)
      implicit integer(i,j)
      implicit character*60(k)
      implicit logical(l)

      include 'common.f'

c..  verbose mode:
      lverbose = .true.

c..  output unit for parameter list (6 = STDOUT)
      iunit = 6

c..  order of calculation:
      iord = 4

c..  strong coupling constant at scale mz (5 active flavors):
      alphasmz = 0.118d0

c..  use MS-bar or pole quark mass? (.true. == MS-bar mass)
      lmsbar = .false.

c..  masses
      massc = 1.65d0      ! charm
      massb = 4.75d0      ! bottom
      masst = 175.d0      ! top

c..  renormalization scale:
      mu = dsqrt(scms)

c..  decoupling scales:
      muc = 2.d0*massc    ! charm
      mub = massb         ! bottom
      mut = masst        ! top

c..  threshold for open quark production
      thrc = 4.8d0
      thrb = 11.2d0
      thrt = 2*masst+10.d0
```



```

c..  lower bound of quark threshold region
      thrclow = 3.73d0
      thrblow = 10.52d0
      thrtlow = 2*masst-10.d0

c..  minimum allowed cms energy:
      sqmin    = 1.8d0

c..  some switches
      lmassless = .false.      ! use only massless approximation
      lqed      = .true.       ! QED corrections (.true. = ON)
      lpsup     = .true.       ! include power suppressed terms
      la3m2     = .true.       ! \alpha_s^3 * m^2 terms
      la3m4     = .true.       ! \alpha_s^3 * m^4 terms
      la3sing   = .true.       ! singlet contribution at order \alpha_s^3
      la4m2     = .true.       ! \alpha_s^4 * m^2 terms

      return
      end

```

D Implementation of running and decoupling

Determination of α_s . rhad contains several routines which cover the consistent running and decoupling of the strong coupling $\alpha_s^{(n_f)}(\mu)$ (in this context see also Refs. [31, 18]).

`runalpha(api0,mu0,mu,inf,inloop,verb,apiout):`

`api0:` $\alpha_s^{(n_f)}(\mu_0)/\pi$

`mu0:` μ_0

`mu:` μ

`inf:` n_f

`inloop:` number of loops used for QCD β function

`verb:` 0=quiet, 1=verbose

`apiout:` $\alpha_s^{(n_f)}(\mu)/\pi$

Evaluates $\alpha_s^{(n_f)}(\mu)$ from $\alpha_s^{(n_f)}(\mu_0)$ by solving numerically the renormalization group equation

`decalpha(als,massth,muth,inf,inloop,idir,alsout):`

`inf:` n_i

`massth:` M_h , heavy quark mass to be decoupled

`muth:` μ^{th}

`inloop:` k_{ord}

`idir:` $\delta \in \{-1, 1\}$

als: $\alpha_s^{(n_i)}$
alsout: $\alpha_s^{(n_i+\delta)}$

Evaluates $\alpha_s^{(n_i+\delta)}(\mu^{\text{th}})$ from $\alpha_s^{(n_i)}(\mu^{\text{th}})$. The order of the matching relations is determined by k_{ord} ($0 \leq k_{\text{ord}} \leq 3$). The matching coefficients require the pole quark mass as input.

rundecalalpha(als0,mu0,mu1,alsout):

mu0: μ_0

mu1: μ_1

als0: $\alpha_s^{(n_i)}(\mu_0)$, where n_i is defined in the subroutine **parameters**

alsout: $\alpha_s^{(n_f)}(\mu_1)$, where n_f is determined with the help of the variables **thrc**, **thrb** and **thrt**

Determines $\alpha_s^{(n_f)}(\mu_1)$ from $\alpha_s^{(n_i)}(\mu_0)$, including decoupling and matching, by calling **decalpha** and **runalpha**. The value for $n_i = \text{infini}$ is set in the subroutines **parameters**. $n_f = \text{inffin}$ is determined according to the value of **mu1** and becomes part of the **common**-block.

In addition there is the subroutine **decalphams** which works analogously to **decalpha**, except that the matching coefficients are parameterized in terms of $\overline{\text{MS}}$ quark masses.

Determination of $\bar{m}_Q(\sqrt{s})$.

runmass(mass0,api0,apif,inf,inloop,massout):

mass0: $\bar{m}_Q(\mu_0)$

api0: $\alpha_s(\mu_0)/\pi$

apif: $\alpha_s(\mu_f)/\pi$

inf: n_f

inloop: number of loops

massout: $\bar{m}_Q(\mu_f)$

Evaluates $\bar{m}_Q^{(n_f)}(\mu)$ from $\bar{m}_Q^{(n_f)}(\mu_0)$ using Eq. (12).

decmassms(mq,als,massth,muth,inf,inloop,idir,mqout):

mq: $\bar{m}_Q^{(n_i)}(\mu^{\text{th}})$

als: $\alpha_s^{(n_i)}(\mu^{\text{th}})$

massth: \bar{m}_h , $\overline{\text{MS}}$ value of heavy quark mass to be decoupled

muth: μ^{th} decoupling scale

inf: n_i

idir: $\delta \in \{-1, 1\}$

inloop: k_{ord}

mqout: $\bar{m}_Q^{(n_i+\delta)}(\mu^{\text{th}})$

Evaluates $\bar{m}_Q^{(n_i+\delta)}(\mu^{\text{th}})$ from $\bar{m}_Q^{(n_i)}(\mu^{\text{th}})$. The order of the matching relations is determined by k_{ord} ($0 \leq k_{\text{ord}} \leq 3$). The matching coefficients require the $\overline{\text{MS}}$ quark mass as input.

rundecmass(mq0,inf,mu0,mu1,mqout):

mq0: $\bar{m}_Q^{(n_i)}(\mu_0)$

inf: n_i

mu0: μ_0

mu1: μ_1

mqout: $\bar{m}_Q^{(n_f)}(\mu_1)$

Determines the $\overline{\text{MS}}$ mass $\bar{m}_Q^{(n_f)}(\mu_1)$ from $\bar{m}_Q^{(n_i)}(\mu_0)$, including decoupling and matching, by calling **decmassms** and **runmass**. n_f is determined according to the value of **mu1**.

Note that in **decmassms** and **rundecmass** only those cases are implemented which are needed for **rhad**.

Pole mass versus $\overline{\text{MS}}$ mass. In case the $\overline{\text{MS}}$ quark masses are used as input the numerical values for the pole quark masses, which are needed for certain (double-bubble) contributions as described in Sect. 2, are computed with the help of the routine **mms2mos**.

mms2mos(mms,inf,inloop,mos):

mms: $\bar{m}_Q(\bar{m}_Q)$

inf: number of active flavors

inloop: number of loops used for the conversion

mos: M_Q

Determines the on-shell mass M_Q from the scale-invariant mass $\bar{m}_Q(\bar{m}_Q)$, where the **inloop**-loop relation is used. In practice we use **inloop=iord**. For the conversion also $\alpha_s(\bar{m}_Q)$ is needed which we determine with the help of the subroutines **runalpha** and **decalphams**.

E Analytical results

All results presented in this section are parametrized in terms of pole quark masses denoted by M_Q , M_1 or M_2 . The conversion to the $\overline{\text{MS}}$ formulas can be performed with the help of Eq. (67).

E.1 Analytical results for $R_Q^{(2)}(s)$

In this appendix we list the results for the two-loop contributions to $R(s)$ as they are implemented in `rhad`. They are either known analytically, or in terms of semi-analytical Padé approximants.

The Abelian two-loop contribution reads

$$r_V^F(s, M_Q) = r_V^{F,pa} - 4C_F r_V^{(1)}(s, M_Q), \quad (36)$$

where $r_V^{F,pa}$ is known in the form of Padé approximants [17]. We quote the result based on a [5/5]-Padé approximant:

$$\begin{aligned} r_V^{F,pa} = & C_F^2 \frac{3}{4\pi} \text{Im} \left\{ \frac{i\pi}{48z} \left[(687 + 186z) \sqrt{1 - 1/z} + 216 \ln \frac{1 - \sqrt{1 - 1/z}}{1 + \sqrt{1 - 1/z}} \right] + \frac{(1 + \tilde{\omega})^2}{1 - \tilde{\omega}} \right. \\ & \times \left[2659.1447467995658619093787 + 994.90626341783737509012835 \tilde{\omega} \right. \\ & \quad - 2742.9905230464882915790412 \tilde{\omega}^2 - 779.40067776480109262194206 \tilde{\omega}^3 \\ & \quad \left. + 562.98408428934139747541229 \tilde{\omega}^4 + 132.845153672444424204018458 \tilde{\omega}^5 \right] \\ & \times \left[121.9768095064564342458129488 + 11.5590492918470301261688922 \tilde{\omega} \right. \\ & \quad - 119.511603603837393164213484 \tilde{\omega}^2 - 1.04113850838776740702415214 \tilde{\omega}^3 \\ & \quad \left. \left. + 18.4653468020861357442841578 \tilde{\omega}^4 + \tilde{\omega}^5 \right]^{-1} \right\}, \quad (37) \end{aligned}$$

and

$$z = \frac{1}{1 - v_Q^2}, \quad v_Q = \sqrt{1 - \frac{4M_Q^2}{s}}, \quad \tilde{\omega} = \frac{2}{z} - 1 + 2i \sqrt{\frac{1}{z} - \frac{1}{z^2}}. \quad (38)$$

$r_V^{(1)}$ can be found in Eq. (18).

The non-Abelian contribution can be written in the form [17]

$$r_V^A(s, M_Q) = r_V^{A,pa} + r_V^{A,g}(s, M_Q) \Big|_{\xi=4}, \quad (39)$$

where ξ is the QCD gauge parameter, $r_V^{A,g}$ is the result from the gluonic double-bubble diagram given below and $r_V^{A,pa}$ is again given in terms of a Padé approximant:

$$\begin{aligned}
r_V^{A,pa} &= C_A C_F \frac{3}{4\pi} \text{Im} \left\{ -i\pi \frac{33 - 27z - 6z^2}{8z^2 \sqrt{1 - 1/z}} + (1 + \tilde{\omega})^2 \right. \\
&\times \left[53.56935816521245 + 23.42800818317322 \tilde{\omega} - 28.58891755403711 \tilde{\omega}^2 \right. \\
&\quad \left. \left. - 10.11103466811403 \tilde{\omega}^3 + 0.4266396586616486 \tilde{\omega}^4 \right] \right. \\
&\times \left[19.19224589510177 - 1.767625499084376 \tilde{\omega} - 13.2990319119615 \tilde{\omega}^2 \right. \\
&\quad \left. \left. + 1.00664474828887 \tilde{\omega}^3 + \tilde{\omega}^4 \right]^{-1} \right\}. \tag{40}
\end{aligned}$$

Following Ref. [32], the exact results of the imaginary part of the fermionic and gluonic double-bubble diagram (see Fig. 3 (d) and (e)), r_V^L and $r_V^{A,g}$, respectively, may be written as ($x \in \{L; A, g\}$)

$$r_V^x(s, M_Q) = C_x \left[-\frac{1}{3} \left(R_\infty^x \ln \frac{\mu^2}{s} - R_0^x \right) \frac{r_V^{(1)}(s, M_Q)}{C_F} + R_\infty^x \delta^{(2)} \right], \tag{41}$$

with

$$\begin{aligned}
C_L &= C_F T, \\
C_{A,g} &= C_A C_F, \\
R_\infty^L &= 1, \\
R_0^L &= -\frac{5}{3} + \ln 4, \\
R_\infty^{A,g} &= -\frac{5}{4} - \frac{3}{8} \xi, \\
R_0^{A,g} &= \frac{31}{12} - \frac{3}{4} \xi + \frac{3}{16} \xi^2 + \left(-\frac{5}{4} - \frac{3}{8} \xi \right) \ln 4. \tag{42}
\end{aligned}$$

$r_V^{(1)}$ is defined in (18), whereas $\delta^{(2)}$ was originally calculated in Ref. [7] and reads:

$$\begin{aligned}
\delta^{(2)} = & -\frac{(3-v_Q^2)(1+v_Q^2)}{6} \\
& \times \left\{ \text{Li}_3(p) - 2\text{Li}_3(1-p) - 3\text{Li}_3(p^2) - 4\text{Li}_3(p1+p) - 5\text{Li}_3(1-p^2) + \frac{11}{2}\zeta_3 \right. \\
& + \text{Li}_2(p) \ln\left(\frac{4(1-v_Q^2)}{v_Q^4}\right) + 2\text{Li}_2(p^2) \ln\left(\frac{1-v_Q^2}{2v_Q^2}\right) + 2\zeta_2 \left[\ln p - \ln\left(\frac{1-v_Q^2}{4v_Q}\right) \right] \\
& - \frac{1}{6} \ln\left(\frac{1+v_Q}{2}\right) \left[36 \ln 2 \ln p - 44 \ln^2 p + 49 \ln p \ln\left(\frac{1-v_Q^2}{4}\right) + \ln^2\left(\frac{1-v_Q^2}{4}\right) \right] \\
& \left. - \frac{1}{2} \ln p \ln v_Q \left[36 \ln 2 + 21 \ln p + 16 \ln v_Q - 22 \ln(1-v_Q^2) \right] \right\} \\
& + \frac{1}{24} \left\{ (15 - 6v_Q^2 - v_Q^4) (\text{Li}_2(p) + \text{Li}_2(p^2)) + 3(7 - 22v_Q^2 + 7v_Q^4) \text{Li}_2(p) \right. \\
& - (1 - v_Q)(51 - 45v_Q - 27v_Q^2 + 5v_Q^3) \zeta_2 \\
& + \frac{(1 + v_Q)(-9 + 33v_Q - 9v_Q^2 - 15v_Q^3 + 4v_Q^4)}{v_Q} \ln^2 p \\
& + \left[(33 + 22v_Q^2 - 7v_Q^4) \ln 2 - 10(3 - v_Q^2)(1 + v_Q^2) \ln v_Q \right. \\
& \quad \left. - (15 - 22v_Q^2 + 3v_Q^4) \ln\left(\frac{1 - v_Q^2}{4v_Q^2}\right) \right] \ln p \\
& + 2v_Q(3 - v_Q^2) \ln\left(\frac{4(1 - v_Q^2)}{v_Q^4}\right) \left[\ln v_Q - 3 \ln\left(\frac{1 - v_Q^2}{4v_Q}\right) \right] \\
& + \frac{237 - 96v_Q + 62v_Q^2 + 32v_Q^3 - 59v_Q^4}{4} \ln p - 16v_Q(3 - v_Q^2) \ln\left(\frac{1 + v_Q}{4}\right) \\
& \left. - 2v_Q(39 - 17v_Q^2) \ln\left(\frac{1 - v_Q^2}{2v_Q^2}\right) - \frac{v_Q(75 - 29v_Q^2)}{2} \right\}, \tag{43}
\end{aligned}$$

with $\zeta_2 = \pi^2/6 \approx 1.64493$, $\zeta_3 \approx 1.20206$, and

$$p = \frac{1 - v_Q}{1 + v_Q}.$$

The double-bubble contribution r_V^T can be written in the form

$$r_V^T(s, M_Q) = TC_F \left(\rho^V(M_Q^2, M_Q^2, s) + \rho^R(M_Q^2, M_Q^2, s) + \frac{1}{3} \ln \frac{M_Q^2}{\mu^2} \frac{r_V^{(1)}}{3C_F} \right), \tag{44}$$

where

$$\begin{aligned}
\rho^V(M_Q^2, M_Q^2, s) = & \frac{1}{6} \left[\frac{3 + 10v_Q^2 - 5v_Q^4}{24} \ln^3 p + \frac{-3 + 40v_Q^2 + 16v_Q^4 - 15v_Q^6}{12v_Q^3} \ln^2 p \right. \\
& + \left(\frac{-18 + 234v_Q^2 + 167v_Q^4 - 118v_Q^6}{18v_Q^2} + \frac{-3 - 10v_Q^2 + 5v_Q^4}{2} \zeta_2 \right) \ln p \\
& \left. + \frac{-9 + 510v_Q^2 - 118v_Q^4}{9v_Q} + v_Q(-27 + 5v_Q^2) \zeta_2 \right], \tag{45}
\end{aligned}$$

and

$$\rho^R(M_Q^2, M_Q^2, s) = \frac{1}{3} \int_{4M_Q^2/s}^{(1-2M_Q/\sqrt{s})^2} dy \int_{4M_Q^2/s}^{(1-\sqrt{y})^2} \frac{dz}{z} \left(1 + \frac{2M_Q^2}{sz}\right) \sqrt{1 - \frac{4M_Q^2}{sz}} \mathcal{F}(y, z), \quad (46)$$

with

$$\begin{aligned} \mathcal{F}(y, z) = & \frac{\frac{8M_Q^4}{s^2} + \frac{4M_Q^2}{s}(1-y+z) - (1-y+z)^2 - 2(1+z)y}{1-y+z} \\ & \times \ln \frac{1-y+z - \sqrt{1 - \frac{4M_Q^2}{sy}} \Lambda^{1/2}(1, y, z)}{1-y+z + \sqrt{1 - \frac{4M_Q^2}{sy}} \Lambda^{1/2}(1, y, z)} \\ & - \sqrt{1 - \frac{4M_Q^2}{sy}} \Lambda^{1/2}(1, y, z) \left[1 + \frac{\frac{16M_Q^4}{s^2} + \frac{8M_Q^2}{s} + 4\left(1 + \frac{2M_Q^2}{s}\right)z}{(1-y+z)^2 - \left(1 - \frac{4M_Q^2}{sy}\right) \Lambda(1, y, z)} \right], \end{aligned} \quad (47)$$

$$\Lambda(1, y, z) = 1 + y^2 + z^2 - 2(y + z + yz). \quad (47)$$

Note that $\rho^R(M_Q^2, M_Q^2, s)$ vanishes for $s \leq (4M_Q)^2$.

The numerical integration of Eq. (46) would be a bottle neck of `rhad`. But it turns out that, for $s > (4M_Q)^2$, $r_V^T(s, M_Q)$ is extremely well approximated by the high energy expansion of Ref. [16], and it drastically shortens the running time of `rhad`. Thus we use this expression as the default in `rhad` for $s > (4M_Q)^2$, whereas for $s \leq (4M_Q)^2$ we can safely use Eq. (44) since the double integral does not contribute in this case. For completeness, we list the expansion for r_V^T up to M_Q^{12}/s^6 [16]:

$$\begin{aligned} r_V^T(s, M_Q) = & C_{FT} \left\{ -118 + \zeta_3 + 14L_{s\mu} + M_Q^2 s \left[-132 + 3L_{s\mu} \right] \right. \\ & + (M_Q^2 s)^2 \left[23 + 18\zeta_2 - 10\zeta_3 + 12L_{ms} - 3L_{ms}^2 + (52 - 6L_{ms})L_{s\mu} \right] \\ & + (M_Q^2 s)^3 \left[43 + 3529\zeta_2 + 3509L_{ms} - 769L_{ms}^2 + (-18827 - 1169L_{ms})L_{s\mu} \right] \\ & + (M_Q^2 s)^4 \left[20233288 + 5336\zeta_2 + 167372L_{ms} - 254L_{ms}^2 \right. \\ & \quad \left. + (-98336 - 2036L_{ms})L_{s\mu} \right] \\ & + (M_Q^2 s)^5 \left[-545596750 + 359245\zeta_2 - 115775L_{ms} + 432845L_{ms}^2 \right. \\ & \quad \left. + (-61699675 - 467645L_{ms})L_{s\mu} \right] \\ & + (M_Q^2 s)^6 \left[-92146976480 - 1105\zeta_2 + 346981540L_{ms} + 1893718L_{ms}^2 \right. \\ & \quad \left. + (-84743270 - 30649L_{ms})L_{s\mu} \right] \left. \right\} + \dots, \end{aligned} \quad (48)$$

where $L_{ms} = \ln(M_Q^2/s)$, $L_{s\mu} = \ln(s/\mu^2)$. The ellipse denotes uncalculated higher order terms in M_Q^2/s .

The double-bubble contribution with zero outer mass and inner mass M_2 is given by [9]

$$r_V^{\text{db}}(s, 0, M_2) = C_{\text{FT}} \left[\varrho^V(M_2^2, s) + \theta(s - 4M_2^2) \left(\varrho^R(M_2^2, s) + \frac{1}{4} \ln \frac{M_2^2}{\mu^2} \right) \right], \quad (49)$$

with

$$\begin{aligned} \varrho^R(M_2^2, s) = & \frac{4}{3} (1 - 6x^2) \left[\frac{1}{2} \text{Li}_3(1 - w2) - \frac{1}{2} \text{Li}_3(1 + w2) \right. \\ & + \text{Li}_3(1 + w1 + a) - \text{Li}_3(1 - w1 - a) + \text{Li}_3(1 + w1 - a) - \text{Li}_3(1 - w1 + a) \\ & + \frac{1}{2} \ln(1 + w1 - w) \left\{ \zeta_2 - \frac{1}{12} \ln^2\left(\frac{1+w}{1-w}\right) + \frac{1}{2} \ln^2\left(\frac{a-1}{a+1}\right) \right. \\ & \left. \left. - \frac{1}{2} \ln\left(\frac{1+w}{2}\right) \ln\left(\frac{1-w}{2}\right) \right\} \right] \\ & + \frac{1}{9} a (19 + 46x) (\text{Li}_2(1 + w1 + a) + \text{Li}_2(1 - w1 - a) - \text{Li}_2(1 + w1 - a) - \text{Li}_2(1 - w1 + a) \\ & + \ln(a - 1a + 1) \ln(1 + w1 - w)) \\ & + 4 (1972 + x + x^2) \left(\text{Li}_2\left(-\frac{1+w}{1-w}\right) - \text{Li}_2\left(-\frac{1-w}{1+w}\right) - \ln x \ln\left(\frac{1+w}{1-w}\right) \right) \\ & + 7 (73189 + 7463x + x^2) \ln(1 + w1 - w) - \frac{1}{3} \left(2123108 + \frac{2489}{54} x \right) w, \end{aligned} \quad (50)$$

$$\begin{aligned} \varrho^V(M_2^2, s) = & \frac{2}{3} (1 - 6x^2) \left(\text{Li}_3(A^2) - \zeta_3 - 2\zeta_2 \ln A + \frac{2}{3} \ln^3 A \right) \\ & + \frac{1}{9} (19 + 46x) \sqrt{1 + 4x} (\text{Li}_2(A^2) - \zeta_2 + \ln^2 A) \\ & + \frac{5}{36} \left(\frac{53}{3} + 44x \right) \ln x + \frac{3355}{648} + \frac{119}{9} x, \end{aligned} \quad (51)$$

where

$$x = \frac{M_2^2}{s}, \quad a = \sqrt{1 + 4x}, \quad w = \sqrt{1 - 4x}, \quad A = \frac{\sqrt{1 + 4x} - 1}{\sqrt{4x}}.$$

In the limit $s \gg M_2^2$, the result for $r_V^{\text{db}}(s, 0, M_2)$ reads

$$r_V^{\text{db}}(s, 0, M_2) = C_{\text{FT}} \left(-\frac{11}{8} + \zeta_3 + \frac{1}{4} \ln \frac{s}{\mu^2} + \mathcal{O}\left(\frac{M_2^4}{s^2}\right) \right). \quad (52)$$

Furthermore we need $r_V^{\text{db}}(s, M_1, 0)$ up to the quadratic mass terms which enters the evaluation of $R_c^{(2)}$ in the limit $s > s_b^{\text{thr}}$. It is given by

$$r_V^{\text{db}}(s, M_1, 0) = C_{\text{FT}} \left(-\frac{11}{8} + \zeta_3 + \frac{1}{4} \ln \frac{s}{\mu^2} + \frac{M_1^2}{s} \left(-\frac{13}{2} + 3 \ln \frac{s}{\mu^2} \right) + \mathcal{O}\left(\frac{M_1^4}{s^2}\right) \right). \quad (53)$$

In order to obtain the result for the double-bubble contribution in the limit $M_2^2 \gg s$ one has to perform the decoupling of M_2 from the coupling constant using Eq. (9) and the

one-loop approximation of Eq. (65). Taking into account the full M_1 dependence the result can be cast in the form [11]

$$\begin{aligned}
r_V^{\text{db,h}}(s, M_1, M_2) = & C_F T \frac{s}{45M_2^2} \left[\left(-1 + \frac{12M_1^4}{s^2} + \frac{16M_1^6}{s^3} \right) \ln \frac{1 + \sqrt{1 - \frac{4M_1^2}{s}}}{1 - \sqrt{1 - \frac{4M_1^2}{s}}} \right. \\
& + \left(\frac{22}{5} + \frac{79M_1^2}{5s} + \frac{8M_1^4}{s^2} \right) \sqrt{1 - \frac{4M_1^2}{s}} \\
& \left. + \left(1 + \frac{2M_1^2}{s} \right) \ln \frac{M_2^2}{M_1^2} \sqrt{1 - \frac{4M_1^2}{s}} \right]. \quad (54)
\end{aligned}$$

The expansion of $C_F T \varrho^V$ in the limit $M_2^2 \gg s$ agrees with $r_V^{\text{db,h}}$ for $M_1 = 0$ and reads

$$r_V^{\text{db,h}}(s, 0, M_2) = C_F T \frac{3s}{8M_2^2} \left(\frac{176}{675} + \frac{8}{135} \ln \frac{M_2^2}{s} \right). \quad (55)$$

The massless limits of the above expressions have been given in Eq. (22).

E.2 Analytical results for $R_Q^{(3)}(s)$

This section lists analytical expressions for the three-loop functions defined in Sect. 6. As already mentioned, only the high-energy expansion is known, including quartic mass terms. We write these functions as follows:

$$r_V^{(3)} = r_0^{(3)} + \frac{M_Q^2}{s} r_{V,2}^{(3)} + \left(\frac{M_Q^2}{s} \right)^2 r_{V,4}^{(3)}, \quad \delta r_0^{(3)} = \frac{M_Q^2}{s} r_{0,2}^{(3)} + \left(\frac{M_Q^2}{s} \right)^2 r_{0,4}^{(3)}. \quad (56)$$

The results for the massless terms have been obtained in Ref. [21, 22], the quadratic mass terms in Ref. [23], and the quartic terms in Ref. [24]. Adopting the on-shell scheme for the mass M_Q , we get, for the contributions where the massive quark couples to the external current:

$$\begin{aligned}
r_0^{(3)} = & 87029288 - 1218 \zeta_2 - 11034 \zeta_3 + 2756 \zeta_5 + L_{s\mu} \left(-432148 + 1212 \zeta_3 \right) + 12116 L_{s\mu}^2 \\
& + n_f \left[-7847216 + 116 \zeta_2 + 2629 \zeta_3 - 259 \zeta_5 + L_{s\mu} \left(78572 - 223 \zeta_3 \right) - 1112 L_{s\mu}^2 \right] \\
& + n_f^2 \left[151162 - 118 \zeta_2 - 1927 \zeta_3 + L_{s\mu} \left(-1136 + 29 \zeta_3 \right) + 136 L_{s\mu}^2 \right], \quad (57)
\end{aligned}$$

$$\begin{aligned}
r_{V,2}^{(3)} = & \frac{22351}{12} - \frac{967}{2} \zeta_2 - 16 \zeta_2 \ln 2 + \frac{502}{3} \zeta_3 - \frac{5225}{6} \zeta_5 + 378 L_{ms} - 9 L_{ms}^2 \\
& + L_{s\mu} \left(-\frac{2385}{4} - 132 L_{ms} \right) + \frac{363}{4} L_{s\mu}^2 + n_f \left[-\frac{8429}{54} + 42 \zeta_2 - \frac{466}{27} \zeta_3 + \frac{1045}{27} \zeta_5 \right. \\
& \left. - \frac{52}{3} L_{ms} + 2 L_{ms}^2 + L_{s\mu} \left(\frac{389}{6} + 8 L_{ms} \right) - 11 L_{s\mu}^2 \right] \\
& + n_f^2 \left(\frac{125}{54} - \frac{2}{3} \zeta_2 - \frac{13}{9} L_{s\mu} + \frac{1}{3} L_{s\mu}^2 \right), \quad (58)
\end{aligned}$$

$$\begin{aligned}
r_{V,4}^{(3)} = & \frac{91015}{108} - \frac{76}{9} \ln^4 2 + \frac{2564287}{540} \zeta_2 - \frac{4568}{9} \zeta_2 \ln 2 \\
& - \frac{128}{3} \zeta_2 \ln^2 2 + \frac{56257}{18} \zeta_3 - \frac{1439}{3} \zeta_2 \zeta_3 - \frac{1565}{6} \zeta_4 - \frac{3770}{3} \zeta_5 - \frac{608}{3} a_4 \\
& + L_{ms} \left(-\frac{5536}{3} + 564 \zeta_2 - 24 \zeta_2 \ln 2 + 416 \zeta_3 \right) - \frac{591}{4} L_{ms}^2 + \frac{15}{2} L_{ms}^3 \\
& + L_{s\mu} \left(-\frac{5297}{12} - 1199 \zeta_2 - 572 \zeta_3 - 88 \zeta_2 \ln 2 + \frac{4033}{4} L_{ms} + \frac{165}{2} L_{ms}^2 \right) \\
& + L_{s\mu}^2 \left(\frac{605}{8} - \frac{363}{2} L_{ms} \right) \\
& + n_f \left[-\frac{21011}{216} + \frac{8}{27} \ln^4 2 - \frac{3544}{9} \zeta_2 - \frac{176}{9} \zeta_2 \ln 2 + \frac{32}{9} \zeta_2 \ln^2 2 - \frac{2323}{9} \zeta_3 \right. \\
& + \frac{700}{9} \zeta_4 + \frac{440}{9} \zeta_5 + \frac{64}{9} a_4 + L_{ms} \left(\frac{2419}{12} + \frac{44}{3} \zeta_2 + \frac{16}{3} \zeta_2 \ln 2 + \frac{28}{3} \zeta_3 \right) \\
& - \frac{157}{6} L_{ms}^2 - \frac{2}{3} L_{ms}^3 + L_{s\mu} \left(\frac{1879}{36} + \frac{416}{3} \zeta_2 + \frac{148}{3} \zeta_3 + \frac{16}{3} \zeta_2 \ln 2 \right. \\
& \left. - \frac{361}{3} L_{ms} + 6 L_{ms}^2 \right) + L_{s\mu}^2 \left(-\frac{55}{6} + 22 L_{ms} \right) \left. \right] \\
& + n_f^2 \left[\frac{35}{18} + \frac{25}{3} \zeta_2 + \frac{112}{27} \zeta_3 + L_{ms} \left(-\frac{94}{27} - \frac{8}{3} \zeta_2 \right) + \frac{13}{9} L_{ms}^2 - \frac{2}{9} L_{ms}^3 \right. \\
& \left. + L_{s\mu} \left(-\frac{35}{27} - 4 \zeta_2 - \frac{8}{9} \zeta_3 + 3 L_{ms} - \frac{2}{3} L_{ms}^2 \right) + L_{s\mu}^2 \left(\frac{5}{18} - \frac{2}{3} L_{ms} \right) \right], \tag{59}
\end{aligned}$$

where n_f is the number of active flavors, $a_4 = \text{Li}_4(1/2) \approx 0.517479$, $\zeta_2 = \pi^2/6 \approx 1.64492$, $\zeta_3 \approx 1.20206$, $\zeta_4 = \pi^4/90 \approx 1.08232$, $\zeta_5 \approx 1.03693$, $L_{ms} = \ln(M_Q^2/s)$ and $L_{s\mu} = \ln(s/\mu^2)$. The mass corrections in the case where the massive quark only appears as insertion in gluon lines reads:

$$r_{0,2}^{(3)} = -80 + 60 \zeta_3 + n_f \left(329 - 83 \zeta_3 \right), \tag{60}$$

$$\begin{aligned}
r_{0,4}^{(3)} = & -\frac{4217}{48} + 15 \zeta_2 + \frac{139}{3} \zeta_3 + \frac{50}{3} \zeta_5 + L_{ms} \left(\frac{97}{4} - 38 \zeta_3 \right) - 2 L_{ms}^2 \\
& + L_{s\mu} \left(-\frac{143}{6} + 22 \zeta_3 + \frac{11}{2} L_{ms} \right) \\
& + n_f \left[\frac{457}{108} - \frac{2}{3} \zeta_2 - \frac{22}{9} \zeta_3 + L_{ms} \left(-\frac{13}{18} + \frac{4}{3} \zeta_3 \right) + L_{s\mu} \left(\frac{13}{9} - \frac{1}{3} L_{ms} - \frac{4}{3} \zeta_3 \right) \right]. \tag{61}
\end{aligned}$$

E.3 Analytical results for $R_Q^{(4)}(s)$

With the help of the renormalization group equation the logarithmic contributions of the massless order α_s^4 result can be reconstructed exactly. Thus, for $\mu^2 \neq s$ Eqs. (33) and (34)

take the form

$$\begin{aligned}
\bar{r}_0^{(4),0L}(s) &= -186 + \left(-\frac{520175}{192} + \frac{3993}{32}\zeta_2 + \frac{38643}{16}\zeta_3 - \frac{3025}{8}\zeta_5 \right) L_{s\mu} \\
&\quad + \left(\frac{49775}{128} - \frac{3993}{16}\zeta_3 \right) L_{s\mu}^2 - \frac{1331}{64}L_{s\mu}^3, \\
\bar{r}_0^{(4),1L}(s) &= 21.3 + \left(\frac{188521}{384} - \frac{363}{16}\zeta_2 - \frac{9695}{24}\zeta_3 + \frac{275}{6}\zeta_5 \right) L_{s\mu} \\
&\quad + \left(-\frac{2263}{32} + \frac{363}{8}\zeta_3 \right) L_{s\mu}^2 + \frac{121}{32}L_{s\mu}^3, \\
r_0^{(4),2L}(s) &= \frac{1045381}{15552} - \frac{593}{432}\pi^2 - \frac{40655}{864}\zeta_3 + \frac{11}{12}\pi^2\zeta_3 + \frac{5}{6}\zeta_3^2 - \frac{260}{27}\zeta_5 \\
&\quad + \left(-\frac{94693}{3456} + \frac{11}{8}\zeta_2 + \frac{257}{12}\zeta_3 - \frac{25}{18}\zeta_5 \right) L_{s\mu} + \left(\frac{593}{144} - \frac{11}{4}\zeta_3 \right) L_{s\mu}^2 - \frac{11}{48}L_{s\mu}^3, \\
r_0^{(4),3L}(s) &= -\frac{6131}{5832} + \frac{11}{432}\pi^2 + \frac{203}{324}\zeta_3 - \frac{1}{54}\pi^2\zeta_3 + \frac{5}{18}\zeta_5 \\
&\quad + \left(\frac{151}{324} - \frac{1}{36}\zeta_2 - \frac{19}{54}\zeta_3 \right) L_{s\mu} + \left(-\frac{11}{144} + \frac{1}{18}\zeta_3 \right) L_{s\mu}^2 + \frac{1}{216}L_{s\mu}^3, \\
\bar{r}_{V,2}^{(4),0L}(s) &= 7110 - \frac{9855433}{864} - \frac{535211}{270}\zeta_2 + \frac{3194}{9}\zeta_2 \ln 2 + \frac{128}{3}\zeta_2 \ln^2 2 + \frac{76}{9}\ln^4 2 - \frac{9655}{18}\zeta_3 \\
&\quad + \frac{1439}{3}\zeta_2\zeta_3 + \frac{1565}{6}\zeta_4 + \frac{18925}{9}\zeta_5 + \frac{608}{3}a_4 \\
&\quad + \left(\frac{178849}{24} - 659\zeta_2 + 56\zeta_2 \ln 2 + \frac{938}{3}\zeta_3 - \frac{5225}{3}\zeta_5 \right) L_{ms} - \frac{2313}{8}L_{ms}^2 + \frac{21}{2}L_{ms}^3 \\
&\quad + \left(-\frac{538849}{32} - \frac{6849}{2}L_{ms} + \frac{297}{4}L_{ms}^2 + \frac{31911}{8}\zeta_2 + 132\zeta_2 \ln 2 - \frac{2761}{2}\zeta_3 \right. \\
&\quad \left. + \frac{57475}{8}\zeta_5 \right) L_{s\mu} + \left(\frac{85437}{32} + \frac{1089}{2}L_{ms} \right) L_{s\mu}^2 - \frac{3993}{16}L_{s\mu}^3, \\
\bar{r}_{V,2}^{(4),1L}(s) &= -1430 + \frac{604967}{648} + \frac{689}{3}\zeta_2 + \frac{76}{3}\zeta_2 \ln 2 - \frac{32}{9}\zeta_2 \ln^2 2 - \frac{8}{27}\ln^4 2 + \frac{10622}{81}\zeta_3 \\
&\quad - \frac{610}{9}\zeta_4 - \frac{8360}{81}\zeta_5 - \frac{64}{9}a_4 + \left(-\frac{35899}{54} + \frac{64}{3}\zeta_2 - \frac{16}{3}\zeta_2 \ln 2 - \frac{1436}{27}\zeta_3 \right. \\
&\quad \left. + \frac{2090}{27}\zeta_5 \right) L_{ms} + \frac{133}{2}L_{ms}^2 - \frac{10}{3}L_{ms}^3 + \left(\frac{713191}{288} - \frac{2353}{4}\zeta_2 - 8\zeta_2 \ln 2 + \frac{4069}{18}\zeta_3 \right. \\
&\quad \left. - \frac{13585}{18}\zeta_5 + 370L_{ms} - 21L_{ms}^2 \right) L_{s\mu} + \left(-\frac{3643}{8} - 66L_{ms} \right) L_{s\mu}^2 + \frac{363}{8}L_{s\mu}^3, \\
r_{V,2}^{(4),2L}(s) &= \frac{114253}{648} - \frac{415}{6}\zeta_2 - \frac{995}{324}\zeta_3 + \frac{53}{9}\zeta_3^2 - \frac{3610}{81}\zeta_5 + \left(\frac{199}{18} + \frac{4}{3}\zeta_2 \right) L_{ms} - \frac{13}{6}L_{ms}^2 \\
&\quad + \frac{2}{9}L_{ms}^3 + \left(-\frac{90835}{864} + \frac{53}{2}\zeta_2 - \frac{233}{27}\zeta_3 + \frac{1045}{54}\zeta_5 - \frac{26}{3}L_{ms} + L_{ms}^2 \right) L_{s\mu} \\
&\quad + \left(\frac{95}{4} + 2L_{ms} \right) L_{s\mu}^2 - \frac{11}{4}L_{s\mu}^3, \\
r_{V,2}^{(4),3L}(s) &= -\frac{2705}{1944} + \frac{13}{18}\zeta_2 + \left(\frac{125}{108} - \frac{1}{3}\zeta_2 \right) L_{s\mu} - \frac{13}{36}L_{s\mu}^2 + \frac{1}{18}L_{s\mu}^3,
\end{aligned}$$

(62)

where the first number in $\bar{r}_0^{(4),0L}$, $\bar{r}_0^{(4),1L}$, $\bar{r}_{V,2}^{(4),0L}$, and $\bar{r}_{V,2}^{(4),1L}$ corresponds to the estimates obtained with the help of the results of Refs. [26, 27].

E.4 Renormalization group coefficients

This section collects the formulas used for the evaluation of the running coupling constant and the $\overline{\text{MS}}$ quark masses. It also contains the conversion formulas for transforming $\overline{\text{MS}}$ quark masses to their on-shell values.

The coefficients of the β -function defined in Eq. (8) read [33]:

$$\begin{aligned}
\beta_0^{(n_f)} &= 14 \left[11 - \frac{2}{3} n_f \right], \\
\beta_1^{(n_f)} &= 116 \left[102 - \frac{38}{3} n_f \right], \\
\beta_2^{(n_f)} &= 164 \left[\frac{2857}{2} - \frac{5033}{18} n_f + \frac{325}{54} n_f^2 \right], \\
\beta_3^{(n_f)} &= 1256 \left[\left(\frac{149753}{6} + 3564 \zeta_3 \right) - \left(\frac{1078361}{162} + \frac{6508}{27} \zeta_3 \right) n_f \right. \\
&\quad \left. + \left(\frac{50065}{162} + \frac{6472}{81} \zeta_3 \right) n_f^2 + \frac{1093}{729} n_f^3 \right]. \tag{63}
\end{aligned}$$

The coefficients of the γ_m -function of Eq. (10) are [34]:

$$\begin{aligned}
\gamma_{m,0}^{(n_f)} &= 1, \\
\gamma_{m,1}^{(n_f)} &= \frac{1}{16} \left[\frac{202}{3} - \frac{20}{9} n_f \right], \\
\gamma_{m,2}^{(n_f)} &= \frac{1}{64} \left[1249 + \left(-\frac{2216}{27} - \frac{160}{3} \zeta_3 \right) n_f - \frac{140}{81} n_f^2 \right], \\
\gamma_{m,3}^{(n_f)} &= \frac{1}{256} \left[\frac{4603055}{162} + \frac{135680}{27} \zeta_3 - 8800 \zeta_5 \right. \\
&\quad \left. + \left(-\frac{91723}{27} - \frac{34192}{9} \zeta_3 + 880 \zeta_4 + \frac{18400}{9} \zeta_5 \right) n_f \right. \\
&\quad \left. + \left(\frac{5242}{243} + \frac{800}{9} \zeta_3 - \frac{160}{3} \zeta_4 \right) n_f^2 + \left(-\frac{332}{243} + \frac{64}{27} \zeta_3 \right) n_f^3 \right]. \tag{64}
\end{aligned}$$

The decoupling coefficient for α_s of Eq. (9) is [35]:

$$\begin{aligned}
(\zeta_g)^2 &= 1 + \frac{\alpha_s^{(n_f)}(\mu)}{\pi} \left(-\frac{1}{6} \ln \frac{\mu^2}{M_h^2} \right) + \left(\frac{\alpha_s^{(n_f)}(\mu)}{\pi} \right)^2 \left(-\frac{7}{24} - \frac{19}{24} \ln \frac{\mu^2}{M_h^2} + \frac{1}{36} \ln^2 \frac{\mu^2}{M_h^2} \right) \\
&\quad + \left(\frac{\alpha_s^{(n_f)}(\mu)}{\pi} \right)^3 \left[-\frac{58933}{124416} - \frac{2}{3} \zeta_2 \left(1 + \frac{1}{3} \ln 2 \right) - \frac{80507}{27648} \zeta_3 - \frac{8521}{1728} \ln \frac{\mu^2}{M_h^2} \right. \\
&\quad \left. - \frac{131}{576} \ln^2 \frac{\mu^2}{M_h^2} - \frac{1}{216} \ln^3 \frac{\mu^2}{M_h^2} + n_l \left(\frac{2479}{31104} + \frac{\zeta_2}{9} + \frac{409}{1728} \ln \frac{\mu^2}{M_h^2} \right) \right], \tag{65}
\end{aligned}$$

and for the quark masses, Eq. (13) [35]:

$$\begin{aligned}
\zeta_m = & 1 + \left(\frac{\alpha_s^{(n_f)}(\mu)}{\pi} \right)^2 \left(\frac{89}{432} - \frac{5}{36} \ln \frac{\mu^2}{M_h^2} + \frac{1}{12} \ln^2 \frac{\mu^2}{M_h^2} \right) + \left(\frac{\alpha_s^{(n_f)}(\mu)}{\pi} \right)^3 \left[\frac{1871}{2916} \right. \\
& - \frac{407}{864} \zeta_3 + \frac{5}{4} \zeta_4 - \frac{1}{36} B_4 + \left(\frac{121}{2592} - \frac{5}{6} \zeta_3 \right) \ln \frac{\mu^2}{M_h^2} + \frac{319}{432} \ln^2 \frac{\mu^2}{M_h^2} \\
& \left. + \frac{29}{216} \ln^3 \frac{\mu^2}{M_h^2} + n_l \left(\frac{1327}{11664} - \frac{2}{27} \zeta_3 - \frac{53}{432} \ln \frac{\mu^2}{M_h^2} - \frac{1}{108} \ln^3 \frac{\mu^2}{M_h^2} \right) \right], \quad (66)
\end{aligned}$$

where $B_4 \approx -1.76280$, $n_l = n_f - 1$ is the number of light (massless) quarks and M_h is the pole mass of the heavy quark. The versions of Eqs. (65) and (66) where the $\overline{\text{MS}}$ mass is used as parameter can be found in Refs. [36, 35, 31, 18].

The conversion from $\overline{\text{MS}}$ to on-shell quark masses reads [3, 4, 5]:

$$\begin{aligned}
\frac{M_Q}{\bar{m}_Q(\mu)} = & 1 + \frac{\alpha_s^{(n_f)}(\mu)}{\pi} \left(\frac{4}{3} + l_{\mu m} \right) + \left(\frac{\alpha_s^{(n_f)}(\mu)}{\pi} \right)^2 \left[\frac{307}{32} + \left(2 + \frac{2}{3} \ln 2 \right) \zeta_2 - \frac{1}{6} \zeta_3 \right. \\
& \left. + \frac{493}{72} l_{\mu m} + \frac{43}{24} l_{\mu m}^2 + n_l \left(-\frac{71}{144} - \frac{1}{3} \zeta_2 - \frac{13}{36} l_{\mu m} - \frac{1}{12} l_{\mu m}^2 \right) \right] \\
& + \left(\frac{\alpha_s^{(n_f)}(\mu)}{\pi} \right)^3 \left[\frac{8481925}{93312} + \zeta_2 \left(\frac{652841}{6480} - \frac{1439}{72} \zeta_3 \right) + \frac{58}{27} \zeta_3 - \frac{3475}{432} \zeta_4 \right. \\
& + \frac{1975}{216} \zeta_5 - \frac{220}{27} a_4 - \frac{575}{27} \zeta_2 \ln 2 - \frac{44}{27} \zeta_2 \ln^2 2 - \frac{55}{162} \ln^4 2 \\
& + l_{\mu m} \left(\frac{177305}{2592} + \frac{37}{3} \zeta_2 - \frac{67}{36} \zeta_3 + \frac{37}{9} \zeta_2 \ln 2 \right) + \frac{19315}{864} l_{\mu m}^2 + \frac{1591}{432} l_{\mu m}^3 \\
& + n_l \left(-\frac{231847}{23328} - \frac{991}{108} \zeta_2 - \frac{241}{72} \zeta_3 + \frac{305}{108} \zeta_4 + \frac{8}{27} a_4 - \frac{22}{27} \zeta_2 \ln 2 \right. \\
& + \frac{4}{27} \zeta_2 \ln^2 2 + \frac{1}{81} \ln^4 2 + l_{\mu m} \left(-\frac{10129}{1296} - \frac{49}{18} \zeta_2 - \frac{7}{9} \zeta_3 - \frac{2}{9} \zeta_2 \ln 2 \right) \\
& \left. - \frac{1103}{432} l_{\mu m}^2 - \frac{10}{27} l_{\mu m}^3 \right) + n_l^2 \left(\frac{2353}{23328} + \frac{13}{54} \zeta_2 + \frac{7}{54} \zeta_3 + l_{\mu m} \left(\frac{89}{648} + \frac{1}{9} \zeta_2 \right) \right. \\
& \left. + \frac{13}{216} l_{\mu m}^2 + \frac{1}{108} l_{\mu m}^3 \right) \left. \right], \quad (67)
\end{aligned}$$

where $a_4 = \text{Li}_4(1/2) \approx 0.517479$, $l_{\mu m} = \ln(\mu^2/\bar{m}_Q^2(\mu))$, and $n_l = n_f - 1$. Other variants of Eq. (67) are listed in Ref. [31].

References

- [1] K.G. Chetyrkin, J.H. Kühn, A. Kwiatkowski, *Phys. Reports* **277** (1996) 189.
- [2] J.H. Kühn, T. Hahn, R. Harlander, arXiv:hep-ph/9912262.
- [3] N. Gray, D.J. Broadhurst, W. Grafe, K. Schilcher, *Z. Phys. C* **48** (1990) 673.

- [4] K.G. Chetyrkin and M. Steinhauser, *Phys. Rev. Lett.* **83** (1999) 4001;
K.G. Chetyrkin and M. Steinhauser, *Nucl. Phys.* **B 573** (2000) 617.
- [5] K. Melnikov and T. van Ritbergen, *Phys. Lett.* **B 482** (2000) 99.
- [6] G. Källén, A. Sabry, *K. Dan. Vidensk. Selsk. Mat.-Fys. Medd.* **29**, 17 (1955);
J. Schwinger, *Particles, Sources and Fields*, Vol. II, (Addison-Wesley, New York, 1973).
- [7] A.H. Hoang, J.H. Kühn, T. Teubner, *Nucl. Phys.* **B 452** (1995) 173.
- [8] K.G. Chetyrkin, A.H. Hoang, J.H. Kühn, M. Steinhauser, T. Teubner, *Eur. Phys. J.* **C 2** (1998) 137.
- [9] A.H. Hoang, M. Jezabek, J.H. Kühn, T. Teubner, *Phys. Lett.* **B 338** (1994) 330.
- [10] A.H. Hoang, T. Teubner, *Nucl. Phys.* **B 519** (1998) 285.
- [11] T. Seidensticker, Diplomarbeit, Universität Karlsruhe, 1998 (unpublished).
- [12] K.G. Chetyrkin, *Phys. Lett.* **B 307** (1993) 169.
- [13] K.G. Chetyrkin, A.L. Kataev, F.V. Tkachov, *Phys. Lett.* **B 85** (1979) 277;
M. Dine, J. Sapirstein, *Phys. Rev. Lett.* **43** (1979) 668;
W. Celmaster, R.J. Gonsalves, *Phys. Rev. Lett.* **44** (1980) 560.
- [14] S.G. Gorishny, A.L. Kataev, S.A. Larin, *Nuovo Cim.* **92A** (1986) 119.
- [15] K.G. Chetyrkin, J.H. Kühn, *Nucl. Phys.* **B 432** (1994) 337.
- [16] K.G. Chetyrkin, R.V. Harlander, J.H. Kühn, M. Steinhauser, *Nucl. Phys.* **B 503** (1997) 339.
- [17] K.G. Chetyrkin, J.H. Kühn, M. Steinhauser, *Phys. Lett.* **B 371** (1996) 93;
Nucl. Phys. **B 482** (1996) 213; *Nucl. Phys.* **B 505** (1997) 40.
- [18] M. Steinhauser, *Phys. Reports* **364** (2002) 247.
- [19] A.L. Kataev, *Phys. Lett.* **B 287** (1992) 209.
- [20] L.R. Surguladze, arXiv:hep-ph/9803211.
- [21] S.G. Gorishny, A.L. Kataev, S.A. Larin, *Phys. Lett.* **B 259** (1991) 144;
L.R. Surguladze, M.A. Samuel, *Phys. Rev. Lett.* **66** (1991) 560, (E) *ibid.* **66** (1991) 2416.
- [22] K.G. Chetyrkin, *Phys. Lett.* **B 391** (1997) 402.
- [23] K.G. Chetyrkin, J.H. Kühn, *Phys. Lett.* **B 248** (1990) 359.
- [24] K.G. Chetyrkin, R.V. Harlander, J.H. Kühn, *Nucl. Phys.* **B 586** (2000) 56; (E) *ibid.* **634** (2002) 413.
- [25] M. Beneke, *Nucl. Phys.* **B 405** (1993) 424.
- [26] P.A. Baikov, K.G. Chetyrkin, J.H. Kühn, *Phys. Rev. Lett.* **88** (2002) 012001.

- [27] P.A. Baikov, K.G. Chetyrkin, J.H. Kühn, *Phys. Lett.* **B 559** (2003) 245.
- [28] A.L. Kataev, V.V. Starshenko, *Mod. Phys. Lett.* **A 10** (1995) 235.
- [29] M.A. Samuel, J.R. Ellis, M. Karliner, *Phys. Rev. Lett.* **74** (1995) 4380;
F. Chishtie, V. Elias, T.G. Steele, *Phys. Rev.* **D 59** (1999) 105013;
K.S. Jeong, T. Lee, *Phys. Lett.* **B 550** (2002) 166.
- [30] P.A. Baikov, K.G. Chetyrkin, J.H. Kühn, *Phys. Rev.* **D 67** (2003) 074026.
- [31] K.G. Chetyrkin, J.H. Kühn, M. Steinhauser, *Comp. Phys. Commun.* **133** (2000) 43.
- [32] K.G. Chetyrkin, A.H. Hoang, J.H. Kühn, M. Steinhauser, T. Teubner, *Phys. Lett.* **B 384** (1996) 233.
- [33] T. van Ritbergen, J.A.M. Vermaseren, S.A. Larin, *Phys. Lett.* **B 400** (1997) 379.
- [34] K.G. Chetyrkin, *Phys. Lett.* **B 404** (161) 1997;
J.A.M. Vermaseren, S.A. Larin, T. van Ritbergen, *Phys. Lett.* **B 405** (1997) 327.
- [35] K.G. Chetyrkin, B.A. Kniehl, M. Steinhauser, *Nucl. Phys.* **B 510** (1998) 61.
- [36] K.G. Chetyrkin, B.A. Kniehl, M. Steinhauser, *Phys. Rev. Lett.* **79** (1997) 2184